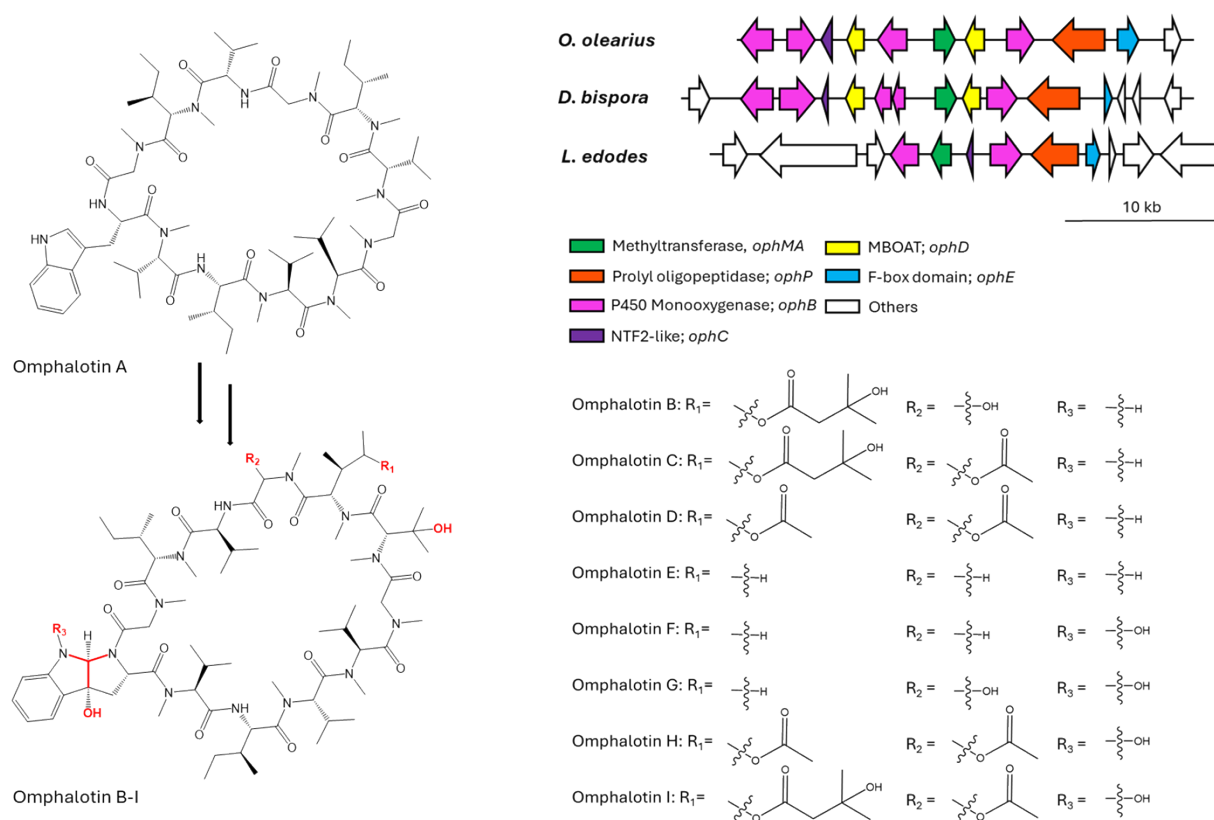


Contents

Figure S1. Conservation of omphalotin-related biosynthetic gene clusters.....	2
Figure S2. OphP production and purification in <i>Pichia pastoris</i>	3
Figure S3. OphP activity towards the chromogenic substrate Z-Gly-Pro-pNA.	4
Figure S4. Susceptibility of <i>in vivo</i> and <i>in vitro</i> production of omphalotin-related peptides towards protease inhibitors.	6
Figure S5. Lack of conversion of completely methylated, full-length OphMA by OphP <i>in vitro</i>	8
Figure S6. Analysis of complex formation between His ₈ OphMA and His ₈ SUMO*OphP	10
Figure S7. HPLC-MS analysis of OphP substrates.....	11
Figure S8. LC-MS/MS spectra of OphP peptide substrates and products.....	13
Figure S9. Activities of OphP, LedP, GmPOPb and ProAlanase towards Oph-5	23
Figure S10. HPLC-MS of macrocyclic OphP peptide products.	25
Figure S11. Preference of OphP for highly methylated peptide substrates by variation of enzyme:substrate ratio.....	26
Figure S12. Preference of OphP for highly methylated peptide substrates by a time course of substrate depletion and product formation.	27
Figure S13. Activities of GmPOPb and OphP towards synthetic peptides PHA1 and AMA1.	32
Figure S14. Overview, relative abundance and LC-MS/MS spectra of macrocyclic peptide products	33
Figure S15. Cartoon and electrostatic surfaces of apo OphP (PDB 7ZB2), apo GmPOPb (PDB 5N4F) and apo human dipeptidyl peptidase IV (DPP-IV, PDB 1NU6).	41
Figure S16. Crystal structure of the OphP:ZPP covalent inhibitor complex.	42
Figure S17. Multiple sequence alignment of OphP with post-proline cleaving prolyl oligopeptidases (POPs).	43
Figure S18. Surface of the P1 pocket of GmPOPb (PDB 5N4C), PCY1 (PDB 5UW6) and OphP (PDB 7ZAZ and 7ZB1)	45
Figure S19. Crystal structures of OphP in complex with Oph-5.	46
Figure S20. ITC experiments between OphP(S580A) and residues from the clasp domain (MPSSLLDAARESGEEASQNGFP), follower peptide (SVMSTE, and VIGSVMSTE), and Oph-5.	47
Figure S21. Production of omphalotin A in <i>P. pastoris</i> and <i>E. coli</i>	48
References	49

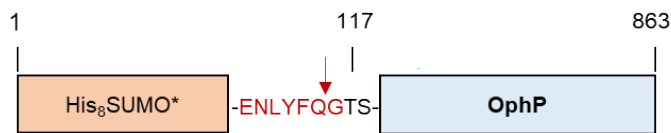
Figure S1. Conservation of omphalotin-related biosynthetic gene clusters. Top right: Schematic representation of the homologous biosynthetic gene clusters from *Omphalotus olearius* (CBS102282, scaffold 137), *Dendrothele bispora* (CBS962.96_v1.0, scaffold 621) and *Lentinula edodes* (Le(bin)0899 ss11, scaffold 10). Genes in the conserved regions of the clusters are shown with colored block arrows. The legend indicates predicted functions or domains of the encoded proteins and the respective protein names in *O. olearius*. NTF2: Nuclear transport factor 2, MBOAT: Membrane bound O-acyltransferase. The DNA scaffolds and gene models were obtained from JGI Mycocosm (<https://mycocosm.jgi.doe.gov/>) for *D. bispora* and *L. edodes*, and from the Syngenta natural products consortium¹ (GenBank PV026309.1) for *O. olearius*. Left and bottom right: Structure of omphalotin variant A and the modifications of variants B-I.



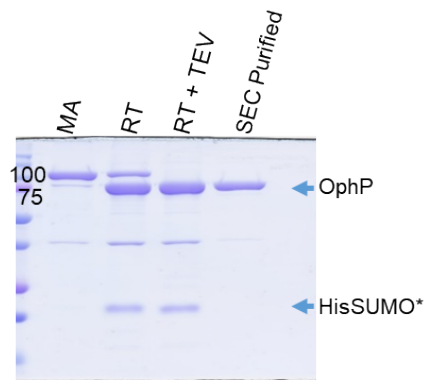
¹ BBSRC-Syngenta Natural Products sLoLa consortium (BB/K002341/1)

Figure S2. OphP production and purification in *Pichia pastoris*. (a) OphP was fused to a His₈-SUMO* via a cleavage site for TEV protease (in red). Residues Thr and Ser after the TEV cleavage site resulted from the insertion of the restriction site *Spe*I between OphP and the tag. The arrow indicates the cleavage site for TEV protease. (b) Purification of OphP. After purification of His₈SUMO*-OphP using metal affinity chromatography (lane MA), the tag was cleaved off by incubation of the purified fusion protein with TEV protease at room temperature (lane RT+TEV). We noted that the tag was also slowly cleaved off even without the addition of TEV protease (lane RT). The P1 site of latter cleavage was mapped to residue Thr117 (a) by whole protein MS. The OphP protein without tag was further purified by size exclusion chromatography (SEC) using an Aekta FPLC system. (c) OphP peak from SEC purification consistent with a monomer. mAU: Milli Absorbance Unit. (d) Heterologous production and purification of OphP homologs LedP and GmPOPb. Recombinant LedP was produced in *P. pastoris* (this study) and GmPOPb in *E. coli*^[1].

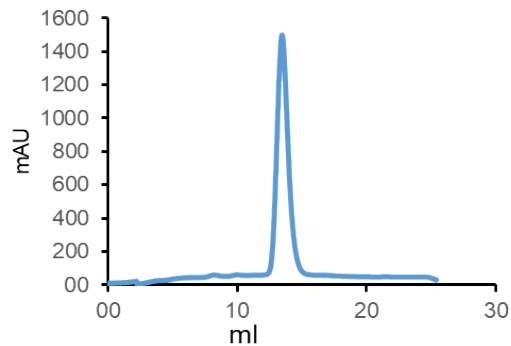
a



b



c



d

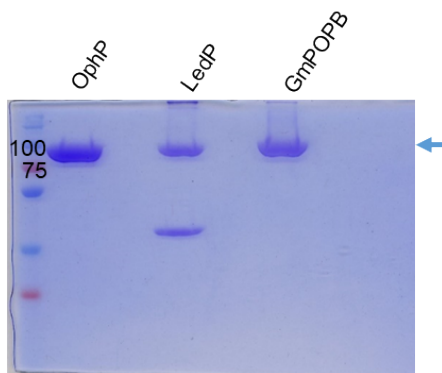
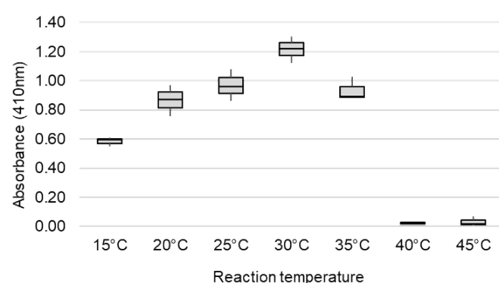
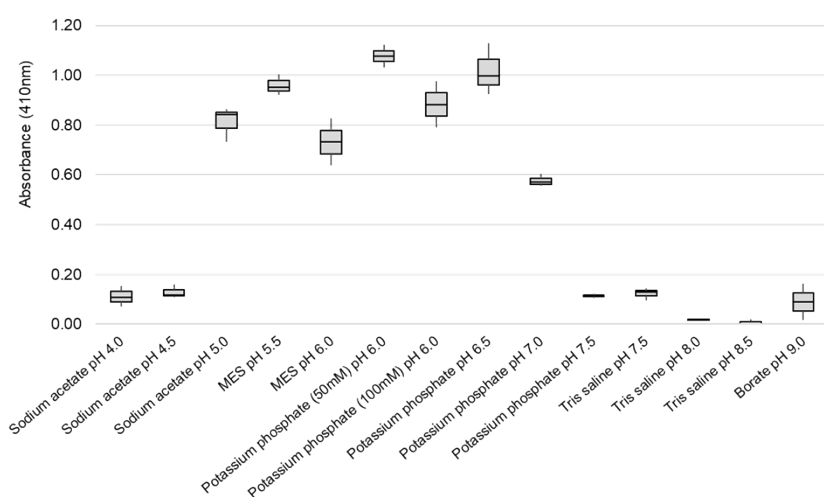


Figure S3. OphP activity towards the chromogenic substrate Z-Gly-Pro-pNA. (a) The effect of temperature. The reactions were run in the standard assay buffer (50 mM HEPES pH 6.0 + 10 mM DTT). (b) The effect of pH (at 30°C). In both assays, (a) and (b), the concentrations of the substrate and the enzyme were 1 mM and 8 μ M, respectively. All assays were performed in triplicates overnight. The enzymatic activity was monitored by measuring the absorbance at 410 nm on an Infinite 200 Pro M Plex spectrophotometer. Error bars indicate standard errors of the mean. (c) Conversion kinetics of Z-Gly-Pro-pNA by OphP. On the left, the calibration curve of pNA, and on the right, enzyme saturation assay are shown. For the substrate calibration curve, the reactions were incubated at 30°C with 8 μ M OphP for 22h. A linear curve was fitted to the data points and the resulting linear equation $A_{410} = \epsilon m \times C + b$ was used to calculate pNA concentration as a function of absorbance ($C = (A - b) / \epsilon m$, where ϵm is the molar extinction coefficient of pNA. The curve was fitted with an R-squared value of 0.9831. For the enzyme saturation assay, pNA product was measured at various times for four different OphP concentrations, 4 μ M (0.5x[Enz]), 8 μ M (1x[Enz]), 16 μ M (2x[Enz]), 40 μ M (5x[Enz]) and 1mM of substrate. The curves for the 2x and 5x relative to substrate concentrations of OphP were outside of the linear range after 4h and 10h, respectively.

a



b



c

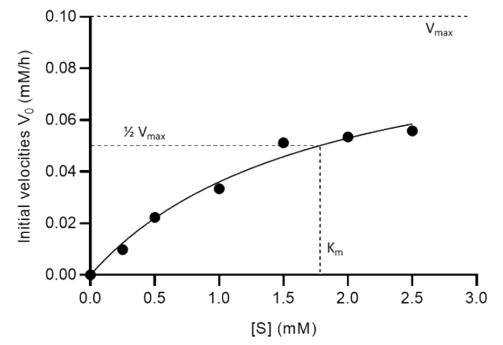
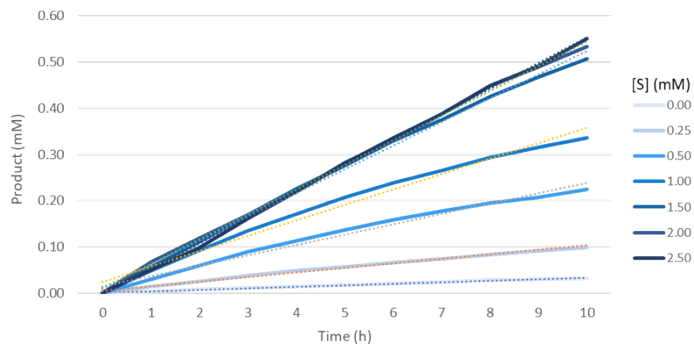
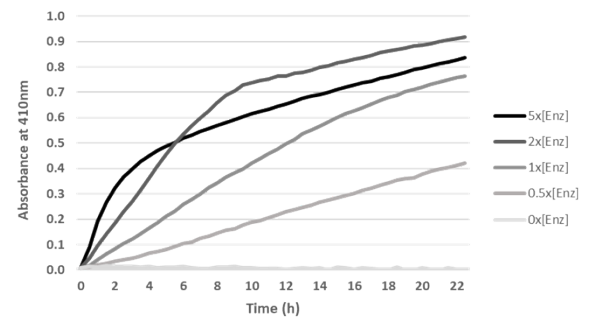
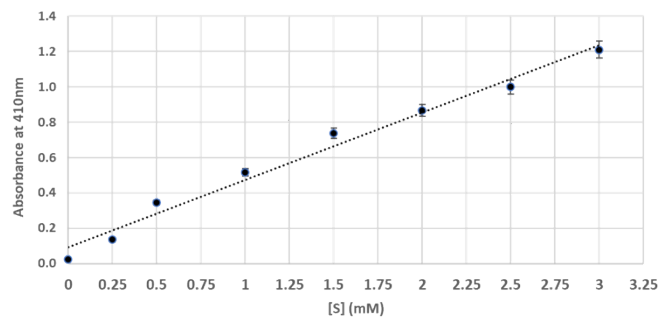
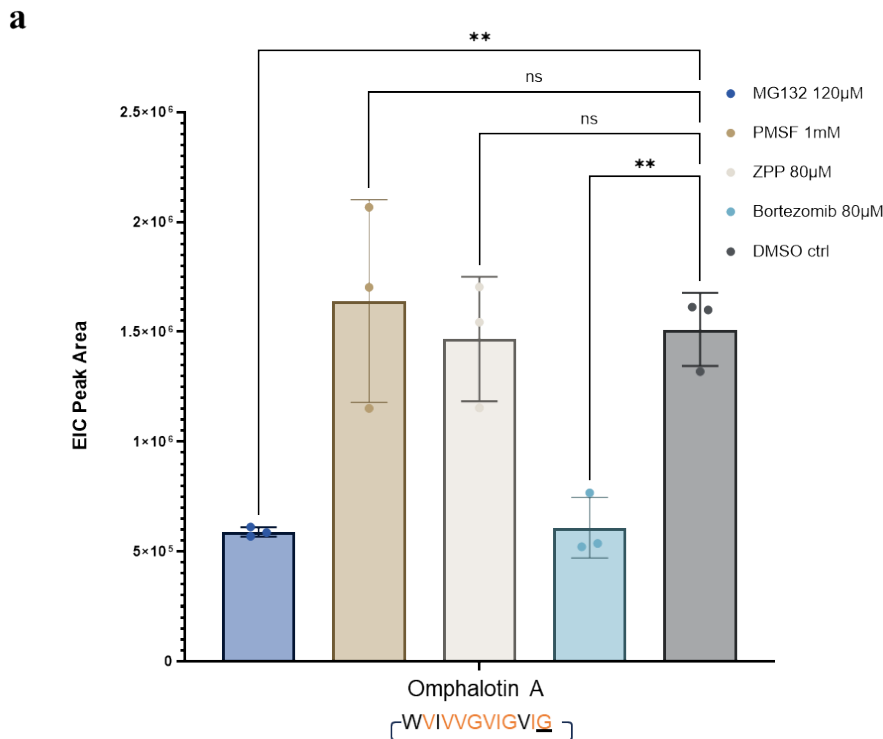


Figure S4. Susceptibility of *in vivo* and *in vitro* production of omphalotin-related peptides towards protease inhibitors. (a) *In vivo* production of omphalotin A in *P. pastoris* co-expressing *ophMA* and *ophP* as described previously^[2], with addition of different protease inhibitors in DMSO at the time of induction of expression. Omphalotin A concentrations were quantified by integrating the Extracted Ion Chromatogram (EIC) peak area of HPLC-MS measurements of cell lysates of triplicate cultures. Ctrl: Control. (b) *In vitro* production of 6- and 7-fold methylated linear and macrocyclic peptide product species with 100 μ M total Oph-5^{high} peptide substrate and 10 μ M OphP concentration, in presence of different protease inhibitors. NOTE: The batch of Oph-5^{high} used for these experiments was the same as used in Figure 3bcd (1:10 batch, see Figure S4a). The reaction was performed in HEPES buffer at pH 7.0 and stopped after 30 minutes. Products were quantified using the EIC peak area of HPLC-MS measurements. (c) *In vitro* production of 6- and 7-fold methylated linear and macrocyclic peptide products with 100 μ M total Oph-5^{high} peptide substrate and 10 μ M OphP enzyme concentration, in presence of two different concentrations of ZPP. The reaction was performed in HEPES buffer at pH 7.0 and stopped after 30 minutes. Peptide species were quantified by integrating the EIC peak area of the HPLC-MS measurements.



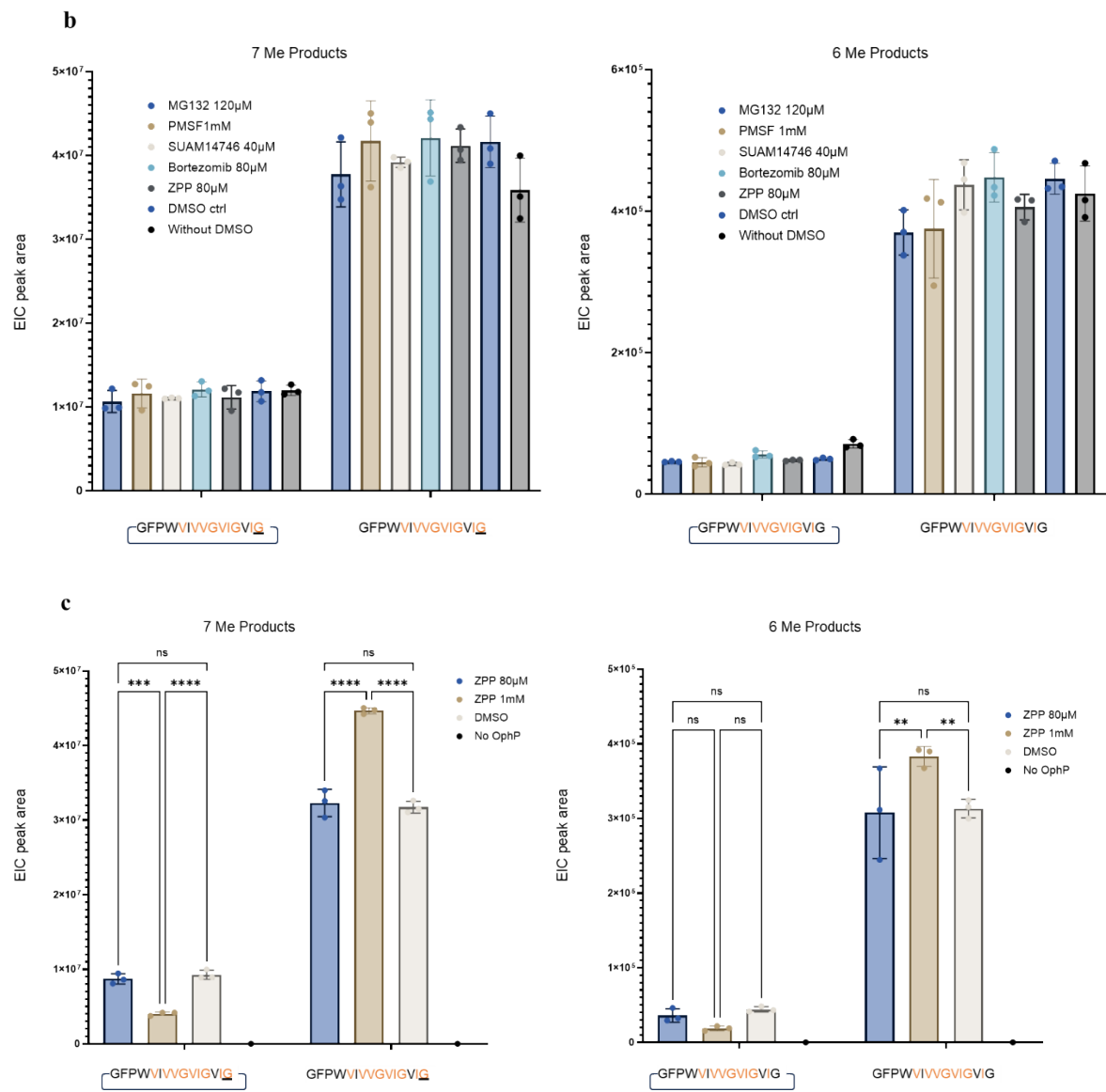
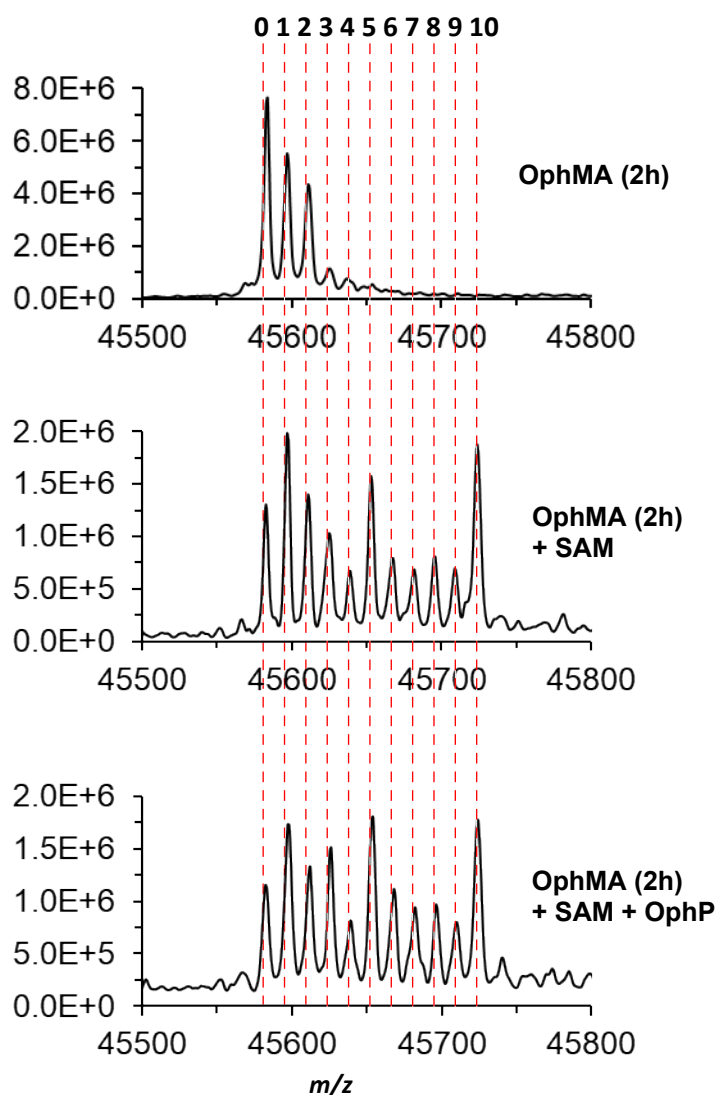


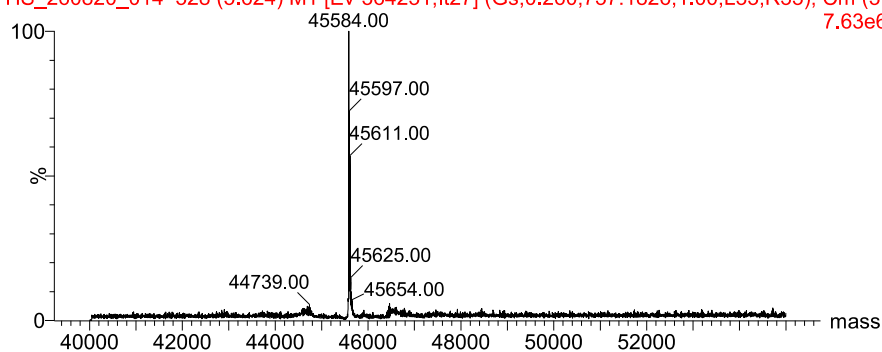
Figure S5. Lack of conversion of completely methylated, full-length OphMA by OphP *in vitro*. (a) ESI-MALDI-ToF analysis of purified OphMA (His₈-tag cleaved off by TEV protease after metal affinity purification from *E. coli* as described in^[3]) coincubated with methyl donor substrate SAM and OphP (His₈SUMO*-tag cleaved off by TEV protease after metal affinity purification from *P. pastoris*) *in vitro*. Full spectra can be found in panels b, c and d. Dashed red lines indicate the various methylation states of OphMA. (b) Intact mass of full length (fl) OphMA expressed in *E. coli* for 2h at 16°C. (c) Intact mass of full length OphMA-2h incubated at 4 mg/ml with 5 mM SAM at room temperature in 50 mM Tris pH 8.0, 100 mM NaCl and 1 mM TCEP for 2h. (d) Intact mass of full length OphMA-2h incubated at 4 mg/ml with 5 mM SAM and 0.9 mg/ml OphP (10 mM) at room temperature in 50 mM Tris pH 8.0, 100 mM NaCl and 1 mM TCEP for 2h. The molecular mass of OphP (after TEV cleavage) is 84611 Da and the peak at 42303 Da corresponds to doubly charged OphP. In panels b, c, d the y axis is the % of the highest signal and the deconvoluted spectrum (thus mass not m/z is used) is shown. The raw data from experiments are shown in red above the spectra.

a

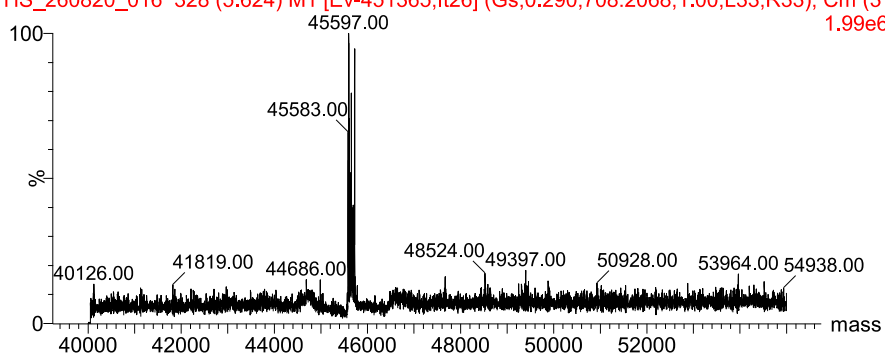


b**OphMA (2h)**

HS_260820_014 328 (5.624) M1 [Ev-364231,It27] (Gs,0.260,737:1826,1.00,L33,R33); Cm (31 7.63e6)

**c****OphMA (2h) + SAM**

HS_260820_016 328 (5.624) M1 [Ev-451365,It26] (Gs,0.290,708:2068,1.00,L33,R33); Cm (31 1.99e6)

**d****OphMA (2h) + SAM + OphP**

HS_260820_018 326 (5.591) M1 [Ev-482669,It29] (Gs,0.290,688:2068,1.00,L33,R33); Cm (31 1.80e6)

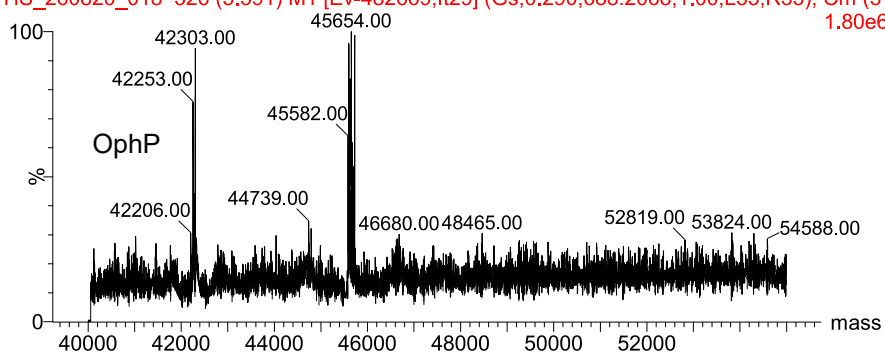


Figure S6. Analysis of complex formation between His₈OphMA and His₈SUMO*OphP(S580A). The two proteins were coexpressed in *Pichia pastoris* GS115 as described in^[2,4] (using pPIC3.5K-His₈-SUMO*-TEVcs-OphP(S580A) instead of pPIC3.5K-His₈-OphP), purified from cell extracts using metal affinity chromatography and analyzed by size exclusion chromatography. (a) Size exclusion chromatography (HiLoad 16/600 Superdex 200 pg) of purified His₈OphMA and His₈SUMO*OphP(S580A). (b) SDS-PAGE of the corresponding fractions from the gel filtration. (c) Intact protein mass determination of His₈OphMA confirming integrity and methylation. The y-axis is the % of the highest signal and the deconvoluted spectrum (thus mass not m/z is used) is shown. The spectrum on the right is a zoom-in of the spectrum on the left. The raw data from experiments are shown in red above the spectra.

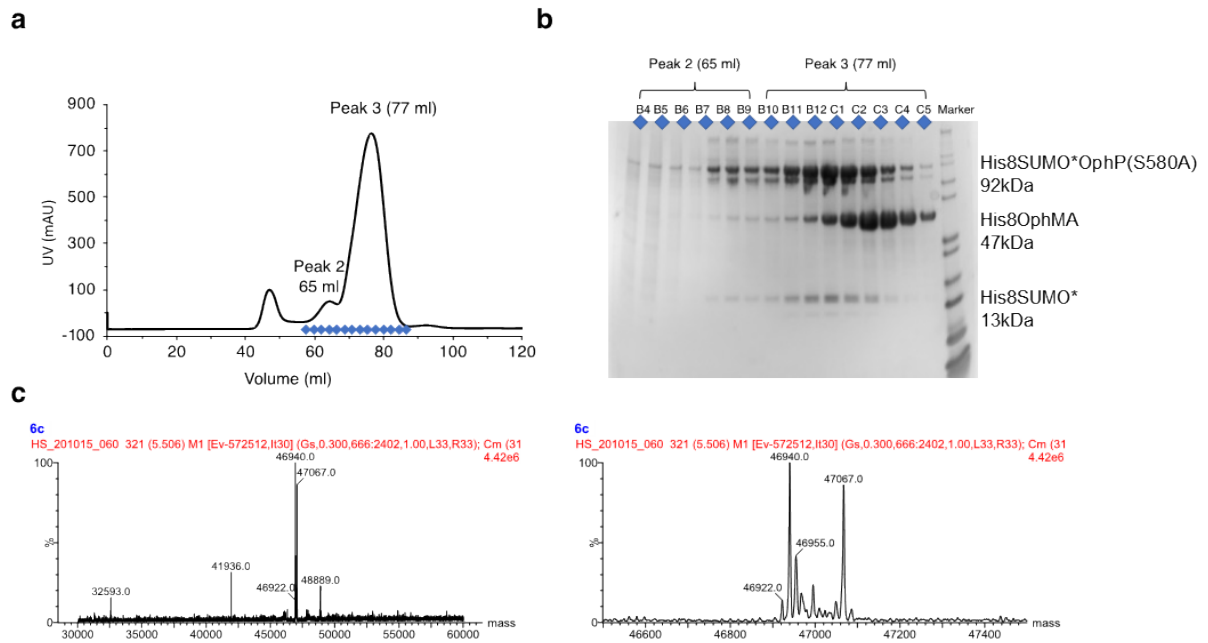


Figure S7. HPLC-MS analysis of OphP substrates. (a, b) Ion chromatograms of OphMA-derived, backbone N-methylated peptide substrates produced using TEV protease-cleavable OphMA-variants and TEV protease only (a) or a combination of TEV protease and GmPOPB (b). The number of methylated residues is indicated by green numbers and red dashed lines to facilitate a comparison. The different peptides have been aligned by extent of methylation rather than by absolute mass. The core peptide is underlined. Note that the follower peptide is different for the non-omphalotin peptides. In case of Oph-5, two different peptide batches with different ratios between 6- and 7-fold methylated species (1:1 and 1:10) were used as substrates. The one with a ratio of 1:10 is labeled ‘Oph-5^{high}’ for the rest of the Supplementary Information.

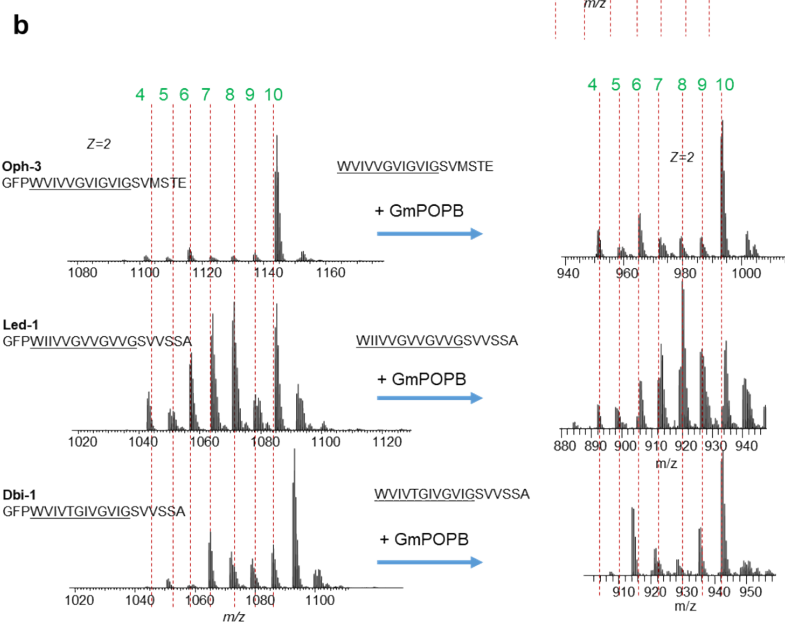
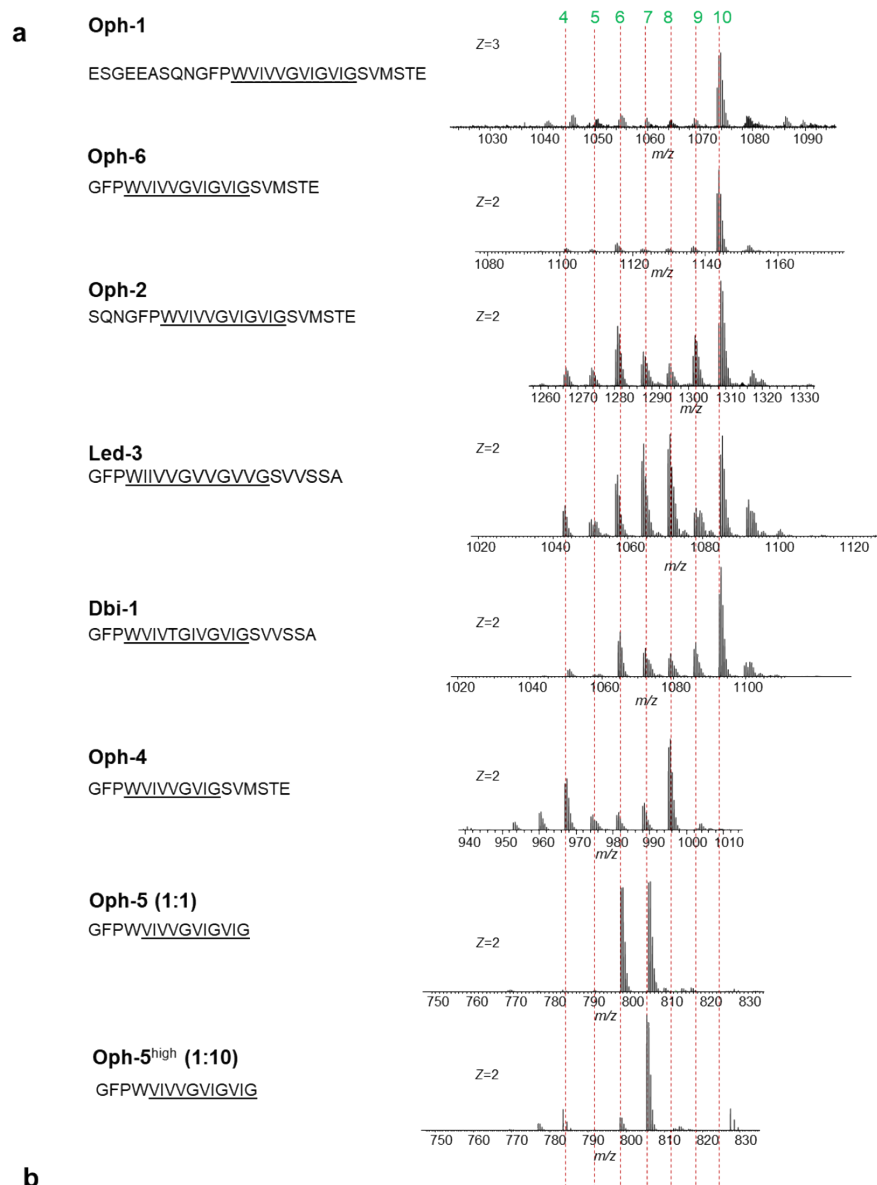
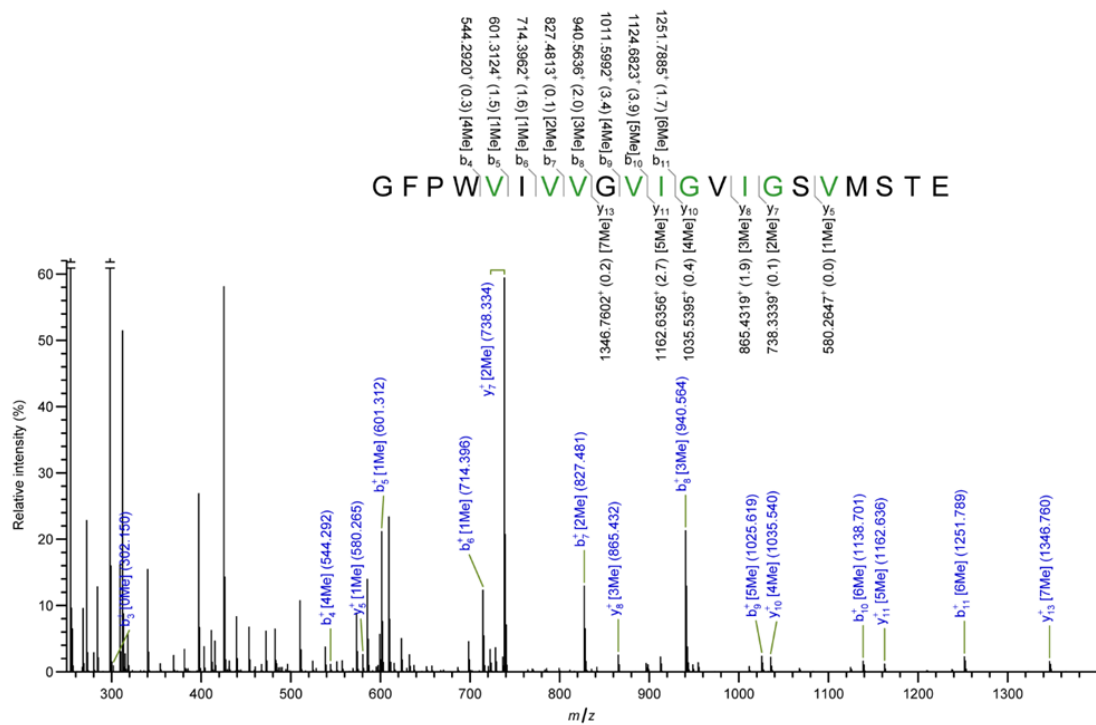
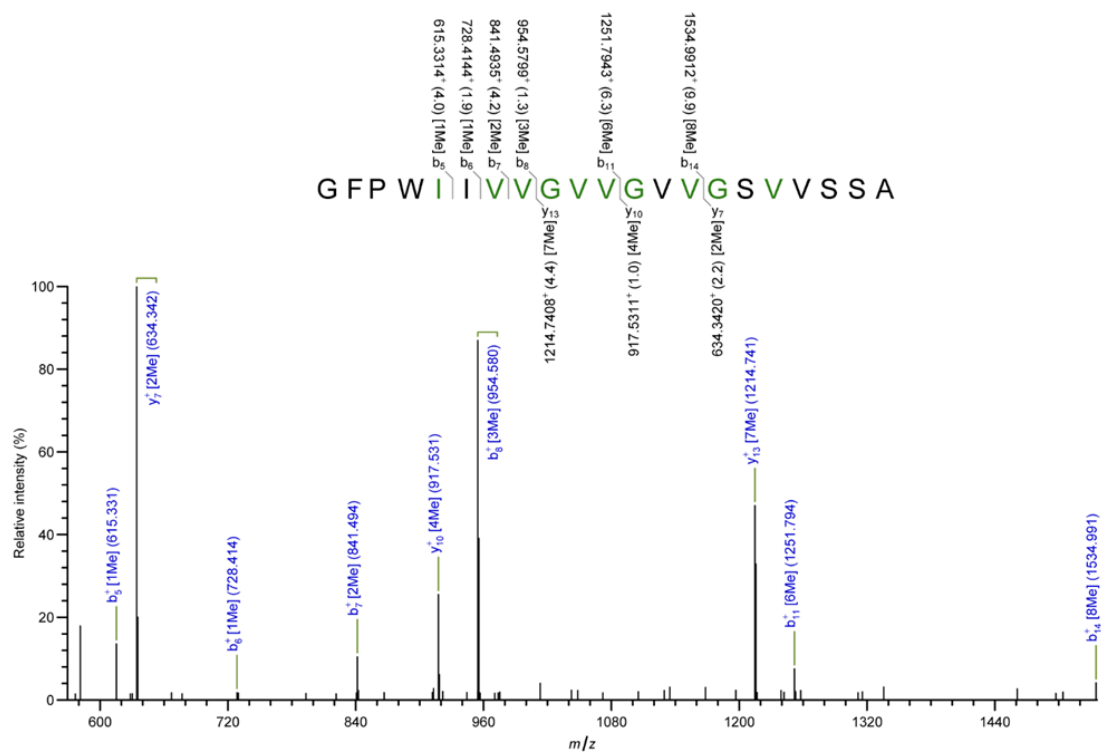


Figure S8. LC-MS/MS spectra of OphP peptide substrates and products. (a-e) Peptide substrates obtained by cleaving OphMA-variants with TEV protease: Oph-3, Led-1, Dbi-1, Oph-6, Oph-4, Oph-2 and Oph-5. (f-l) Linear peptide products obtained by incubation of the peptide substrates with OphP: linear 15mer and 12mer derived from Oph-3 (f-g), linear 12mer and 15mer derived from Led-1 (h-i), 15mer derived from Dbi-1 (j), linear 15mer and 18mer derived from Oph-2 (k-l). (m-o) Linear omphalotin A, lentinulin A and dendrothelin A intermediates. Methylated residues are highlighted in green color. b-ions and y-ions are shown in blue color. Mass tolerance between observed masses and the theoretical masses was set at 10 ppm. This difference is indicated in parentheses. Mass precision was set at 4 decimals. (p) Sequences of OphMA-derived OphP peptide substrates and products produced in this work, with α -N-methylated residues highlighted in orange. Note that methylation by OphMA proceeds from N- to C-terminus and that only the completely methylated forms of the peptides are displayed. The P1 residues recognized by OphP are underlined.

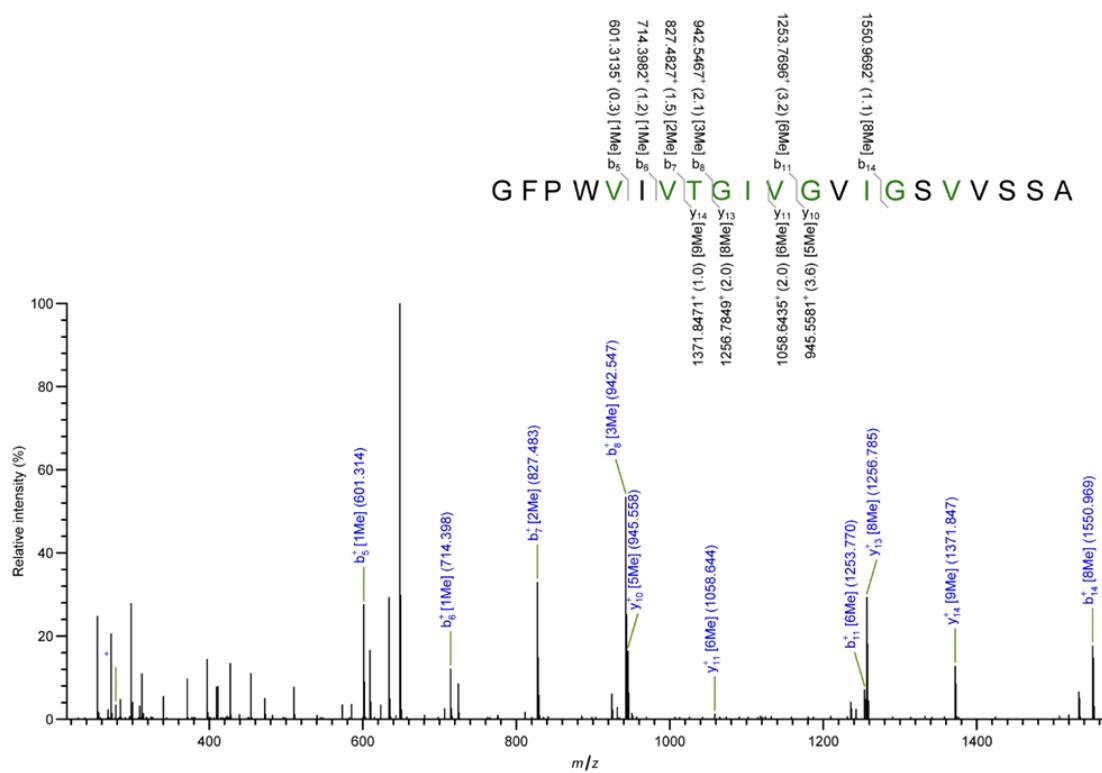
a



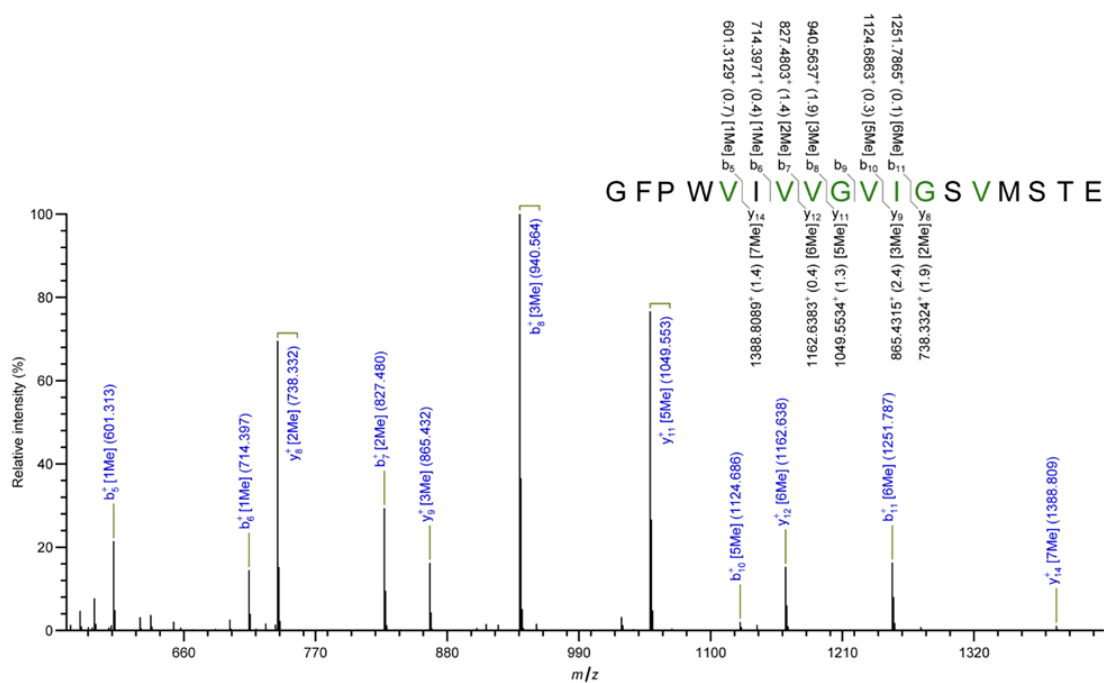
b



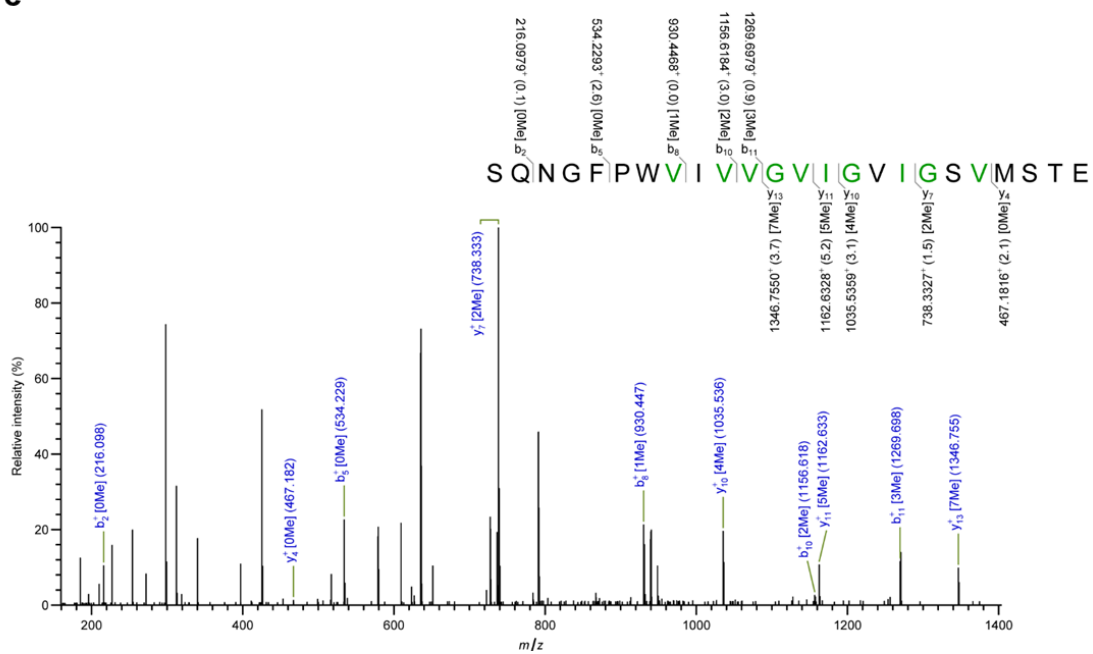
c



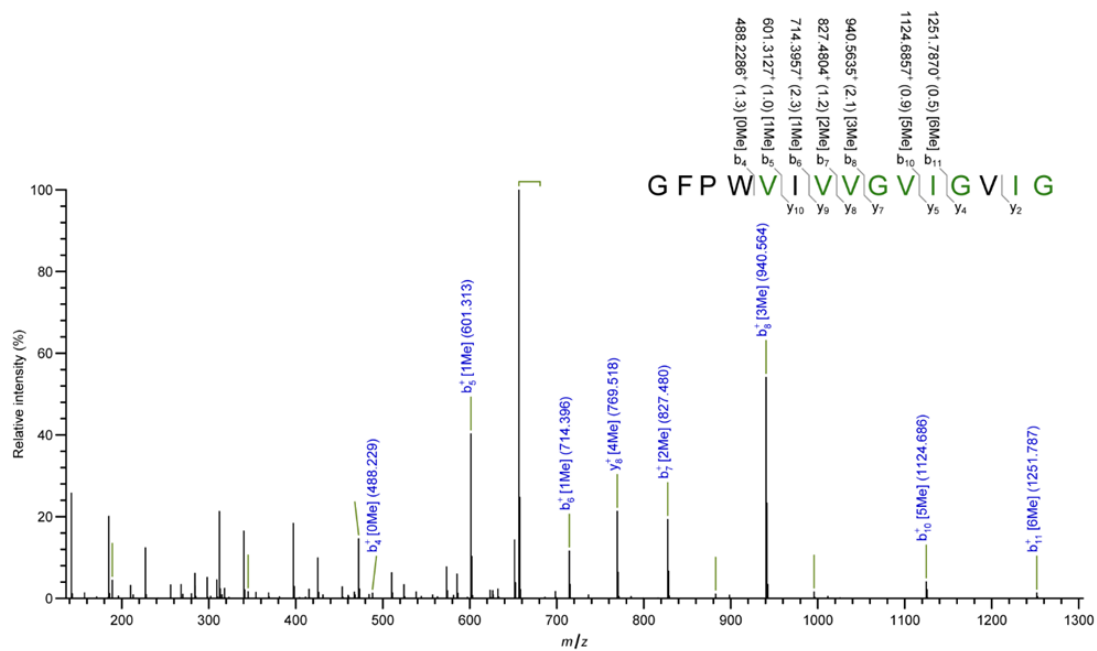
d



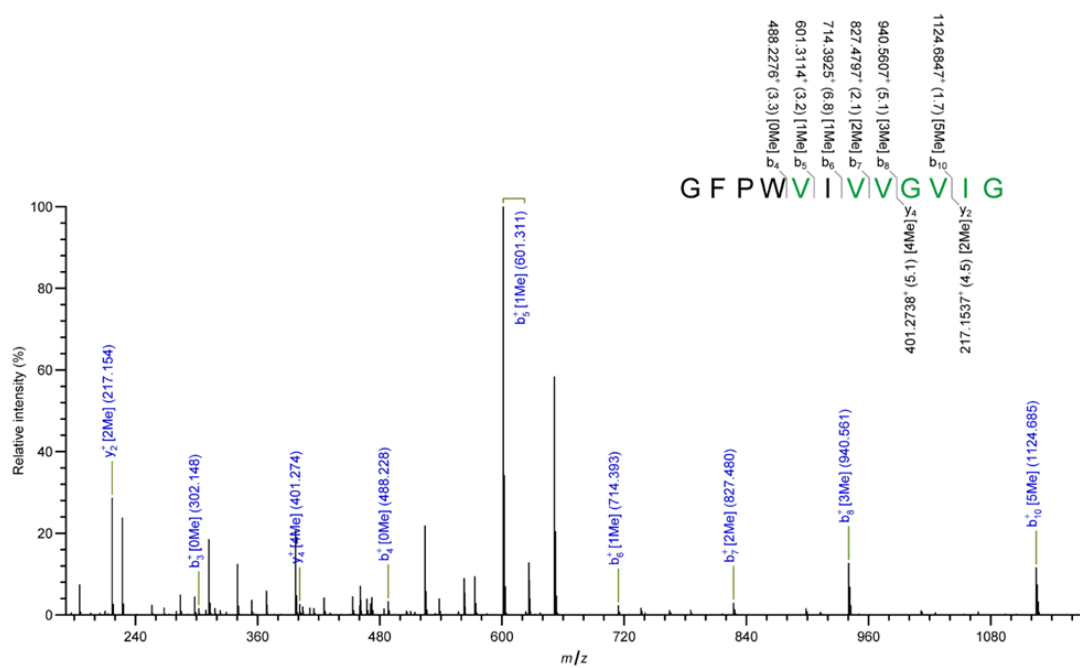
e



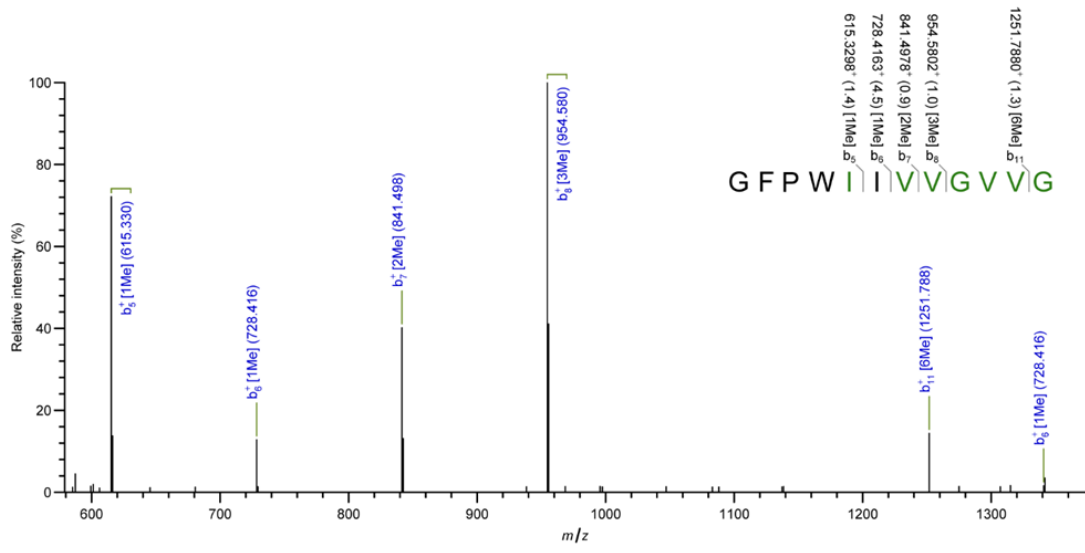
f



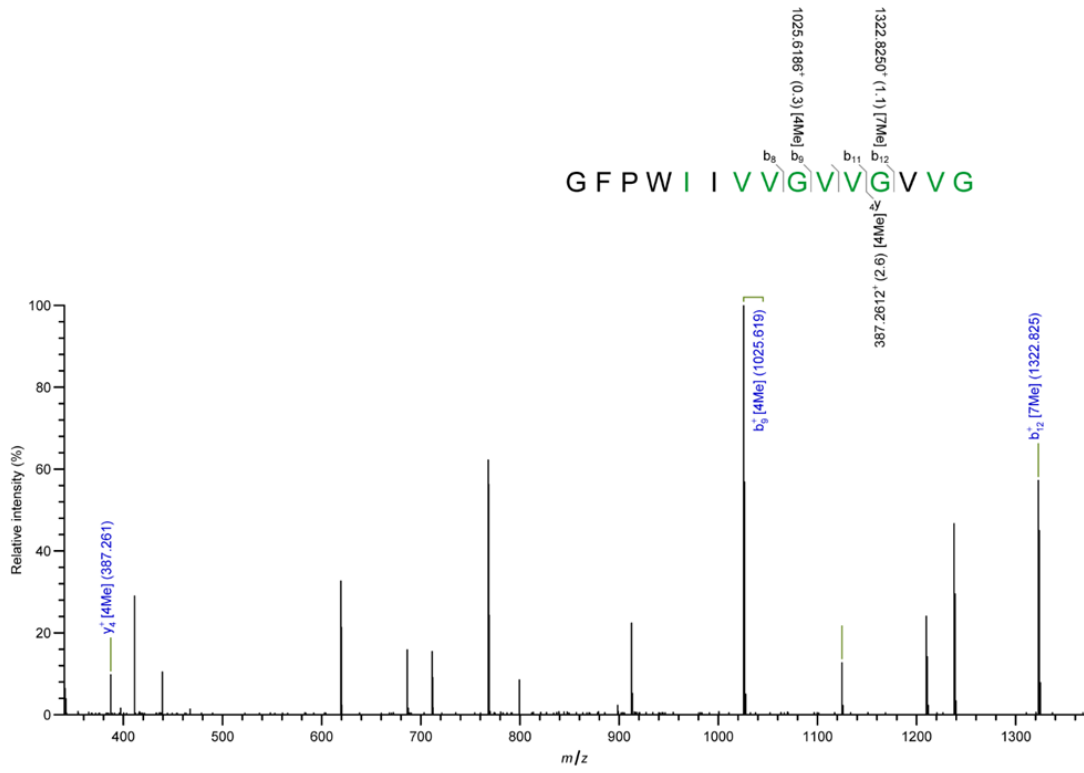
g



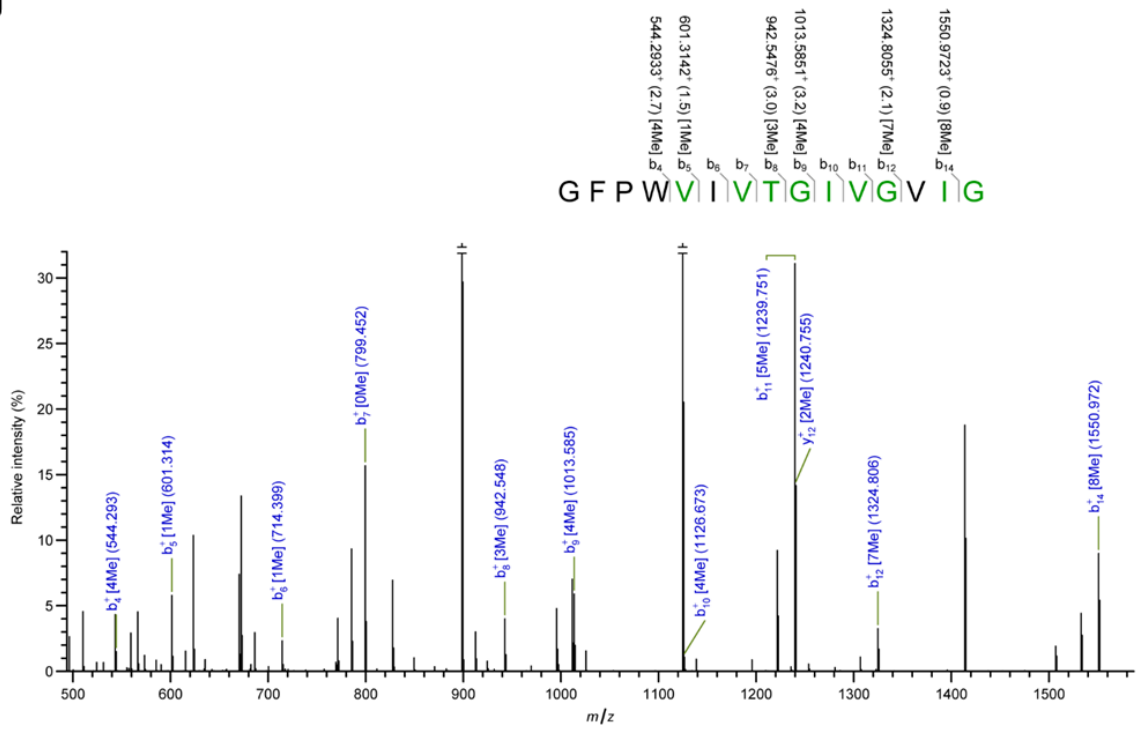
h



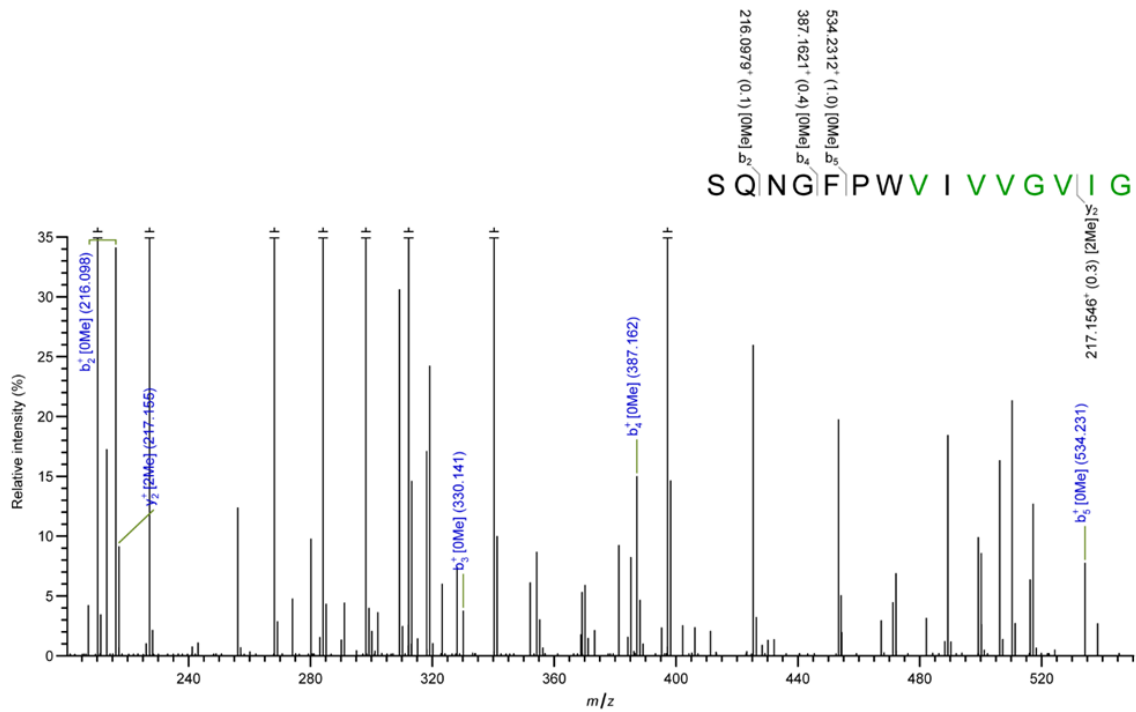
i



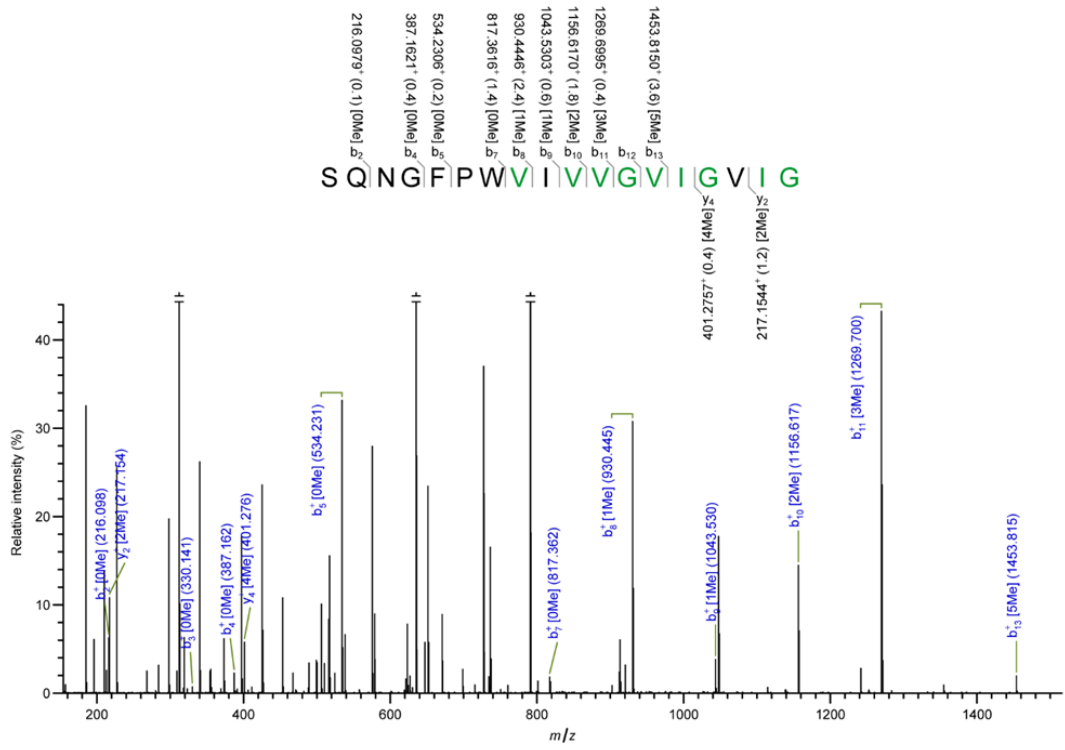
j



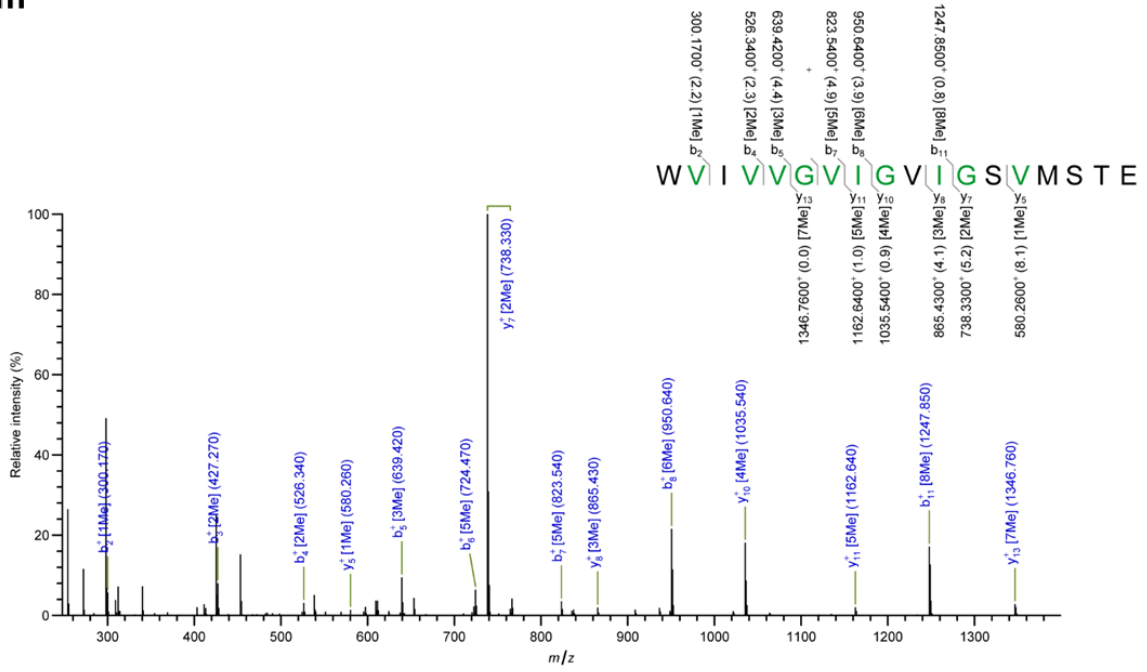
k



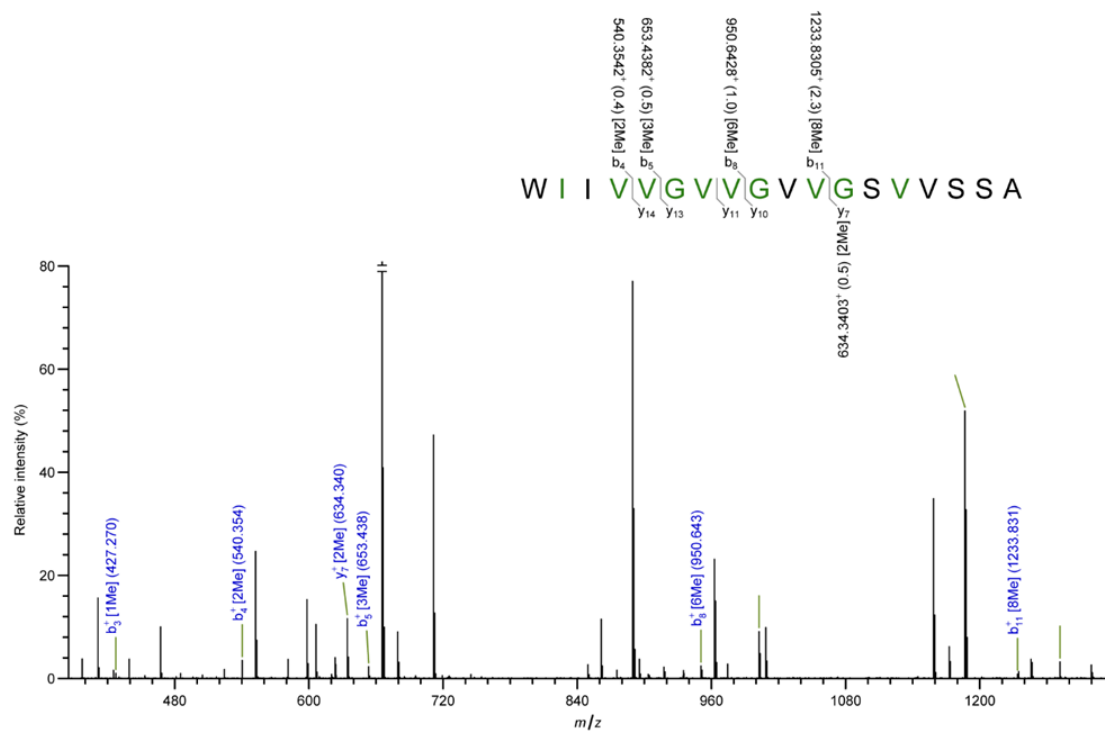
l



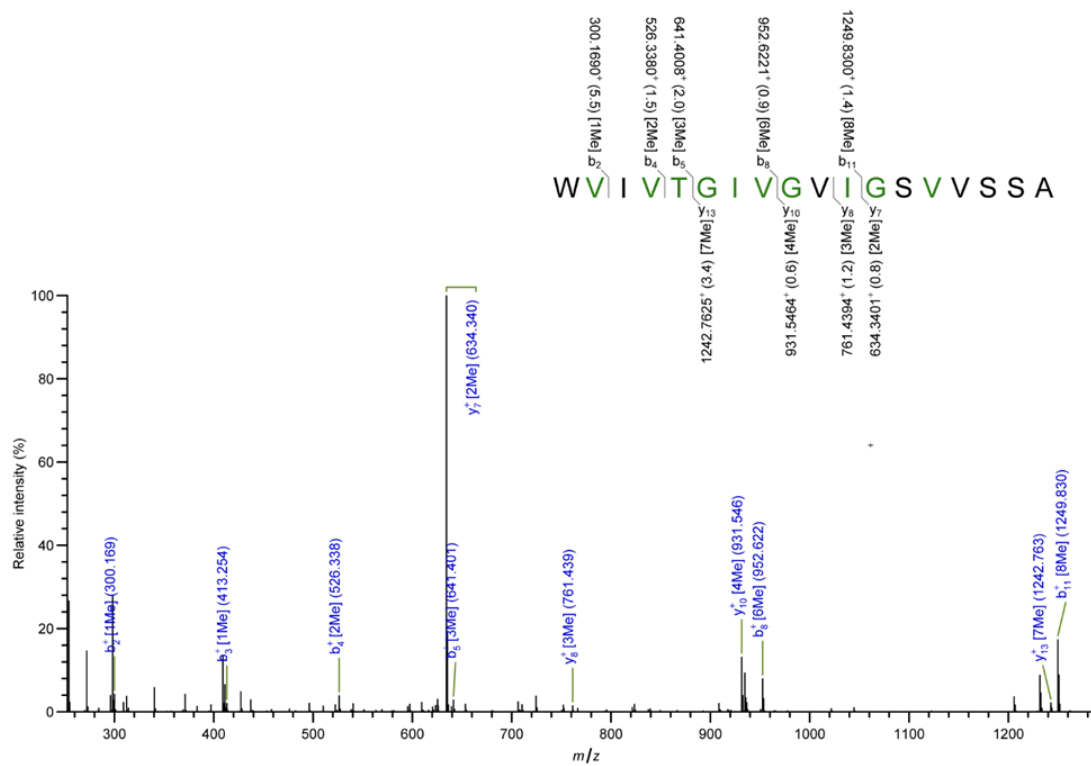
m



n



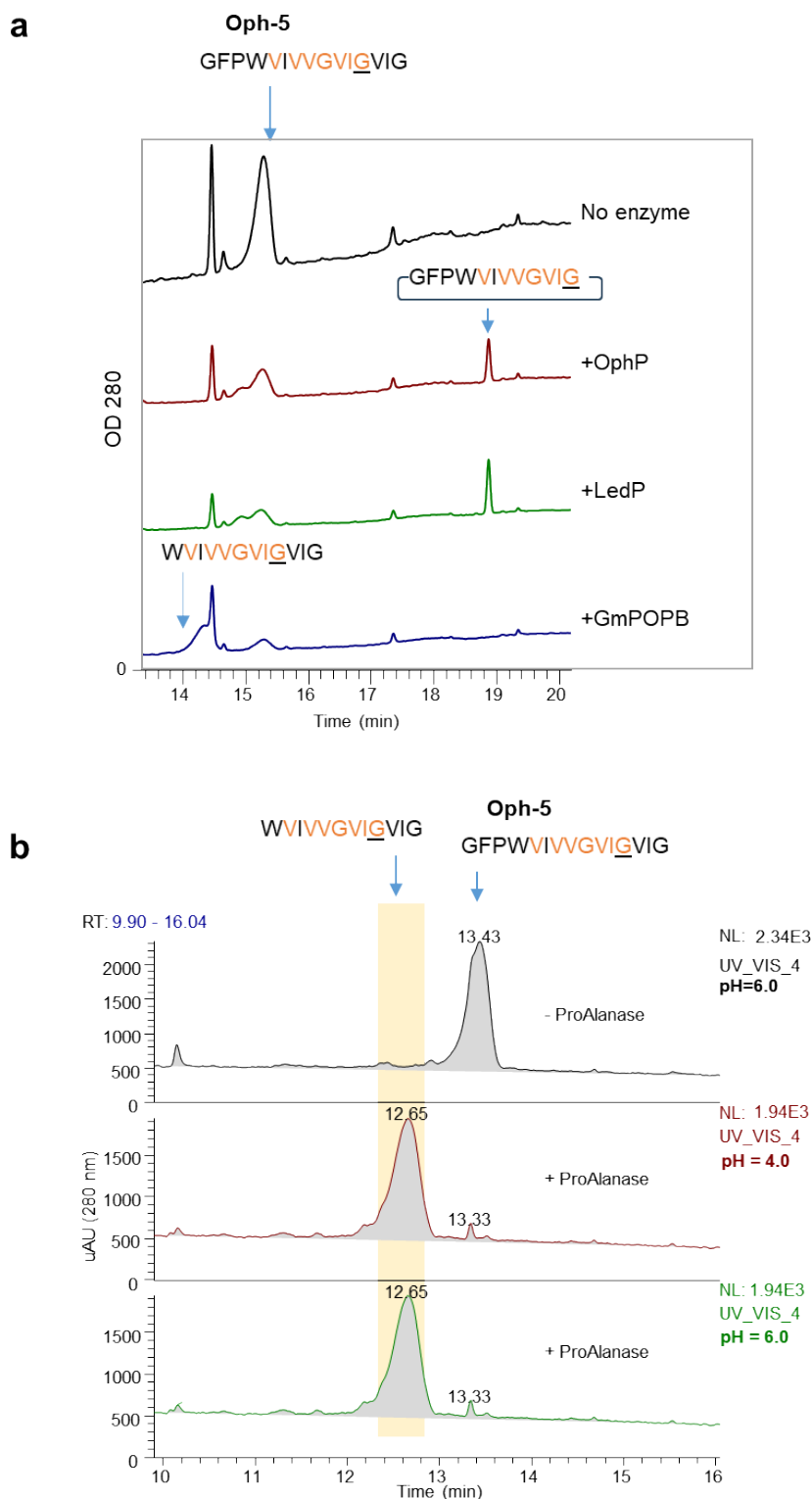
o



p

OphP substrate	Protein/peptide sequence	Linear OphP product(s)	
OphMA (417 aa)	...ESGEEASQNGFPWVIVVGVIQSVSMSTE	None	None
Oph-1	ESGEEASQNGFPWVIVVGVIQSVSMSTE	None	None
Oph-2	SQNGFPWVIVVGVIQSVSMSTE	SQNGFPWVIVVGVIQ SQNGFPWVIVVGVIQ	<u>SQNGFPWVIVVGVIQ</u> <u>SQNGFPWVIVVGVIQ</u>
Oph-3	GFPWVIVVGVIQSVSMSTE	GFPWVIVVGVIQ GFPWVIVVGVIQ	<u>GFPWVIVVGVIQ</u> <u>GFPWVIVVGVIQ</u>
Oph-4	GFPWVIVVGVIQSVSMSTE	GFPWVIVVGVIQ	<u>GFPWVIVVGVIQ</u>
Oph-5	GFPWVIVVGVIQVIG	GFPWVIVVGVIQ	<u>GFPWVIVVGVIQ</u>
Oph-6	WVIVVGVIQSVSMSTE	WVIVVGVIQ WVIVVGVIQ	<u>WVIVVGVIQ</u> (omphalotin A)
Oph-7	WVIVVGVIQSVSMSTE	WVIVVGVIQ	None
Oph-8	WVIVVGVIQVIG	WVIVVGVIQ	None
Led-1	GFPWIIIVGVVGVS SVSSA	GFPWIIIVGVVG GFPWIIIVGVVG	<u>GFPWIIIVGVVG</u> <u>GFPWIIIVGVVG</u>
Dbi-1	GFPWVIVTGIVGVSVSSA	GFPWVIVTGIVGV GFPWVIVTGIVGV	<u>GFPWVIVTGIVGV</u> <u>GFPWVIVTGIVGV</u>
Led-2	WIIIVGVVGVS SVSSA	WIIIVGVVG WIIIVGVVG	<u>WIIIVGVVG</u> (lentinulin A)
Dbi-2	WVIVTGIVGVSVSSA	WVIVTGIVGV WVIVTGIVGV	<u>WVIVTGIVGV</u> (dendrothelin A)

Figure S9. Activities of OphP, LedP, GmPOPB and ProAlanase towards Oph-5 (1:1 batch, see Figure S7a), Oph-6, Led-2 and Dbi-2 . (a) GmPOPB compared to OphP and LedP activities. (b) ProAlanase activity. The enzymatic activity was assessed by determining the UV absorbance at 280 nm. (c) MS-analysis of omphalotin A and its orthologues lentinulin A and dendrothelin A produced from Oph-6, Led-2 and Dbi-2 using OphP. The MS chromatograms show masses of both protonated cyclic peptides and corresponding sodium and ammonium adducts.



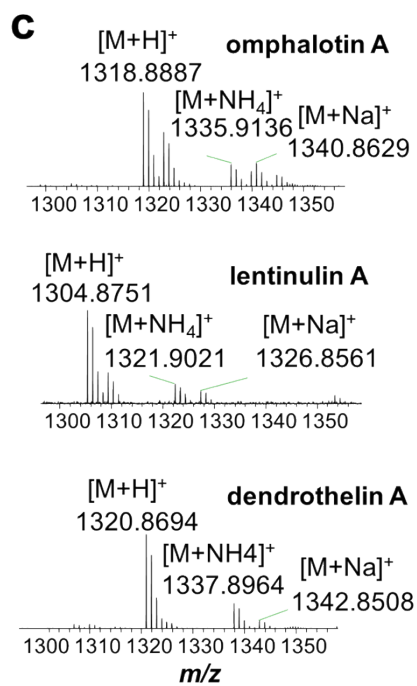


Figure S10. HPLC-MS of macrocyclic OphP peptide products. Extracted ion chromatograms (EICs) of peptide products derived from Led-1 and Dbi-1 by the action of OphP. Methylated residues are highlighted in green. Macrocyclization is indicated by a bracket below the peptide sequence.

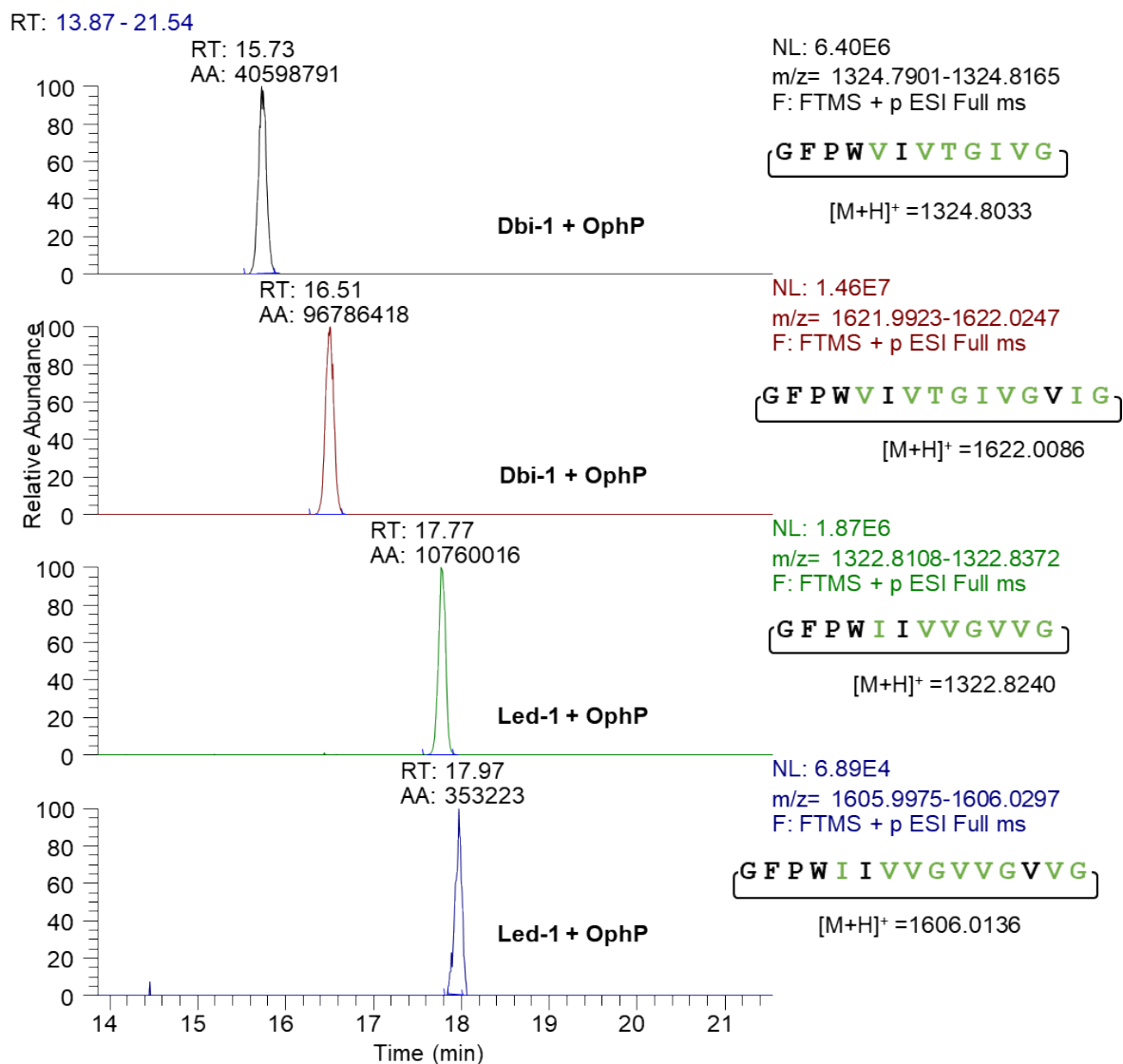


Figure S11. Preference of OphP for highly methylated peptide substrates by variation of enzyme:substrate ratio. The reaction was conducted in the standard buffer [50 mM HEPES pH 7.0, 10 mM DTT] at 30°C, overnight. NOTE: The batch of Oph-5 used for these experiments was the same as used for Figure 3a (1:1 batch, see Figure S4a). **(a)** RP-HPLC UV absorption profile of 100 μ M of Oph-5 with varying concentrations of OphP (0, 1, 2, 5, 10, 20 μ M). Linear products resulting from the peptidase activity of OphP can be detected but overlapped with the starting material. 6-fold methylated cyclo(GFPW^{me}VI^{me}V^{me}V^{me}G^{me}V^{me}IG) can only be detected when high concentrations of OphP are used. Dashed lines show the retention times of the various peptide species. **(b)** Mass spectrometric analysis showing ion chromatograms of the consumption of Oph-5 mixture (100 μ M) when subjected to different concentrations of OphP. The 7-fold methylated Oph-5 is depleted at high concentrations of OphP (10 and 20 μ M).

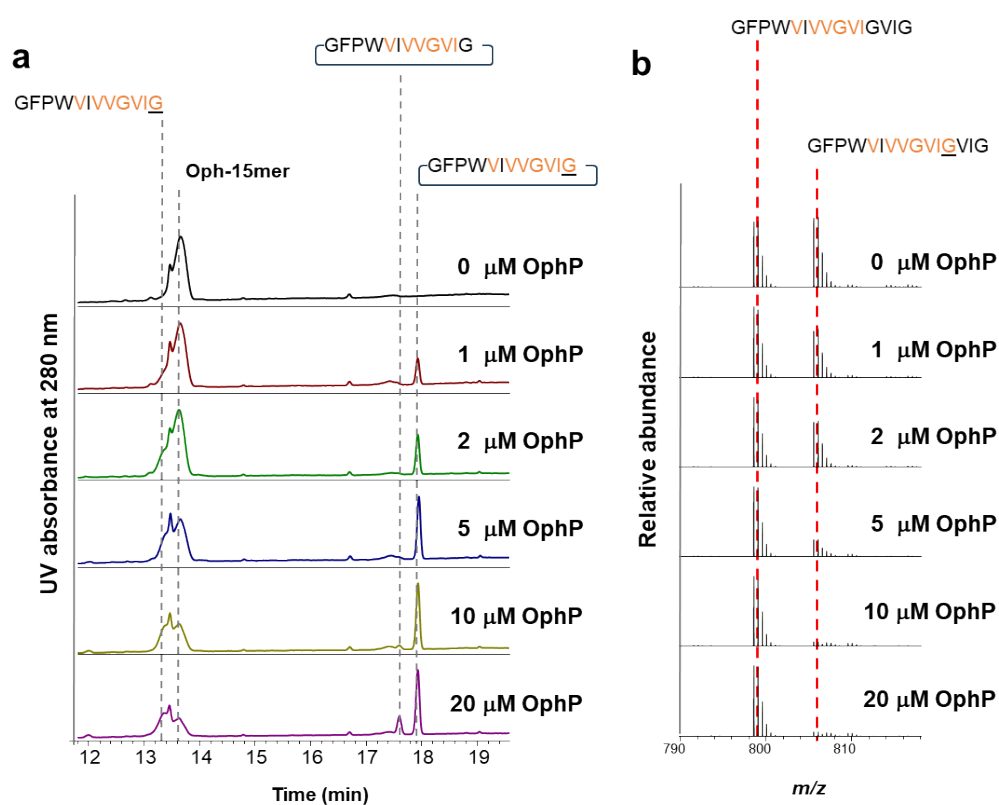
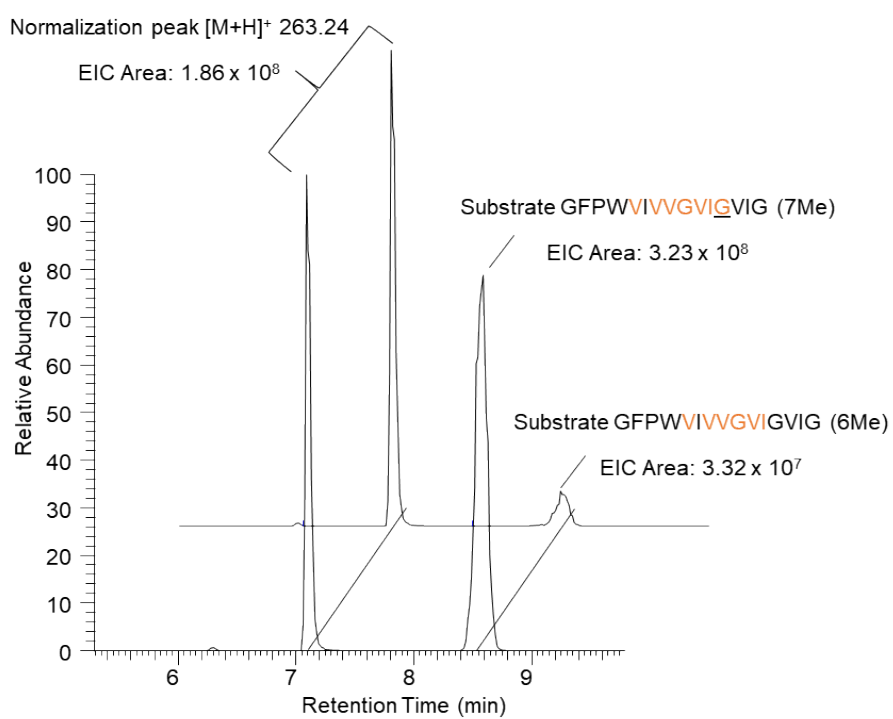
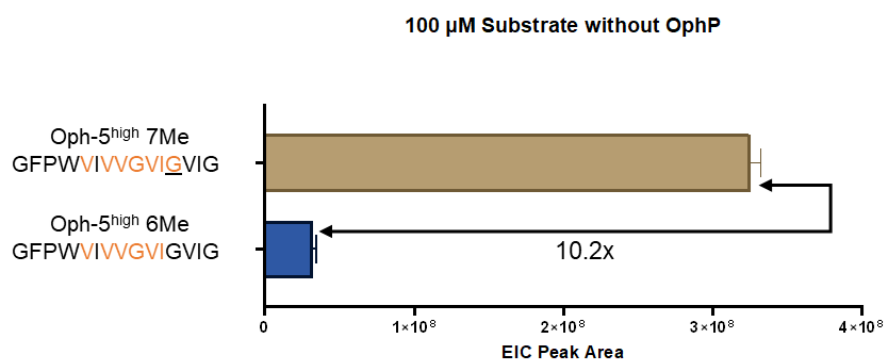
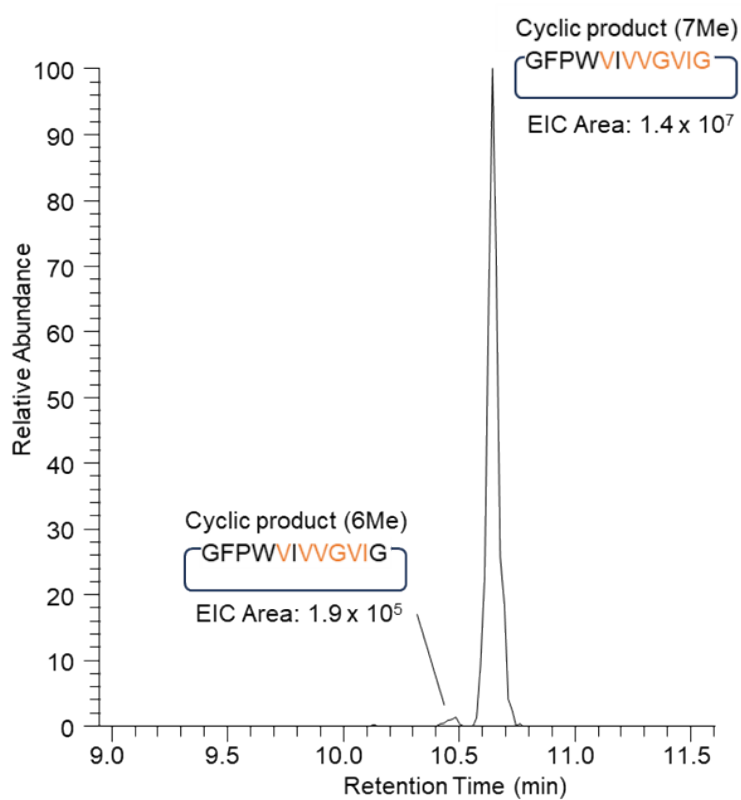
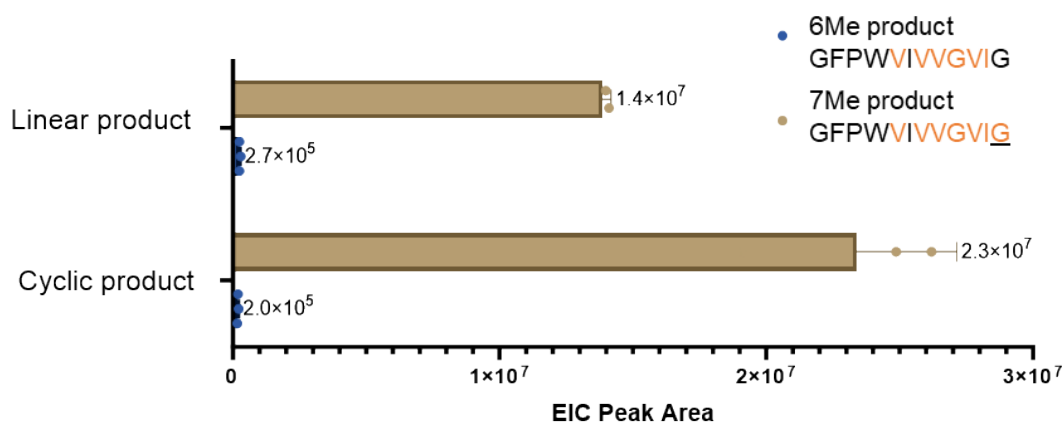
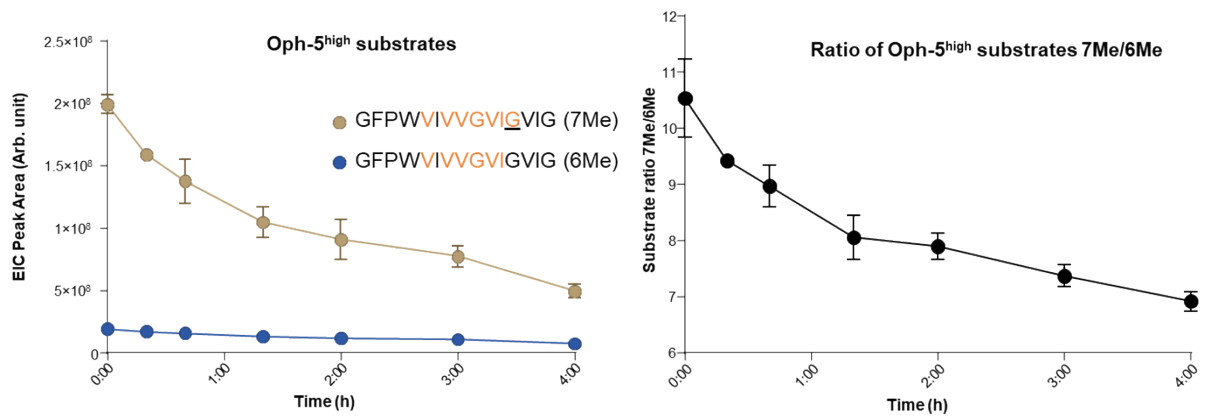
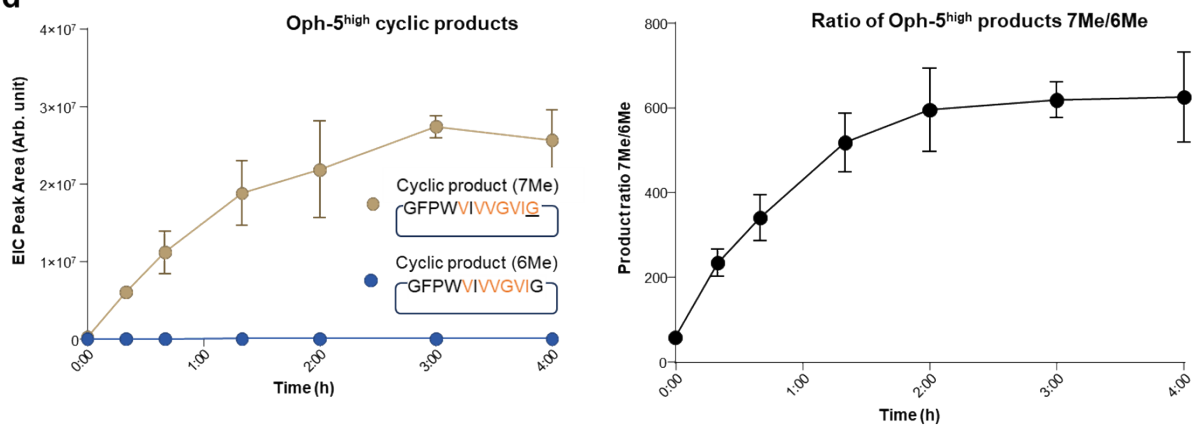


Figure S12. Preference of OphP for highly methylated peptide substrates by a time course of substrate depletion and product formation. NOTE: The batch of Oph-5^{high} used for these experiments was the same as used for Figure 3bcd (1:10 batch, see Figure S4a). **(a,b)** EIC peak area of Oph-5^{high} substrate and product species of 30 min *in vitro* reaction with 10 μ M OphP and Oph-5^{high} substrate (mixture of 6Me and 7Me) in HEPES buffer at pH 7.0. **(a)** Comparison of 6- and 7-fold methylated substrate species at 100 μ M total substrate concentration without addition of OphP. **(b)** Comparison of 6- and 7-fold methylated product species at equimolar (90 μ M) substrate concentration and 10 μ M OphP concentration. **(c-f)** Time course of *in vitro* reaction between 10 μ M OphP and 100 μ M total Oph-5^{high} substrate (mixture of 6Me and 7Me species) in HEPES buffer at pH 7.0. EIC peak areas of 6- and 7-fold methylated peptide substrate **(c)** and product **(d)** species were measured at 8 time points over 4 hours. Left panels in **(c, d)** show the absolute EIC peak areas and the right panels the ratio between the 7- to 6-fold methylated peptide species over the 7 time points. A batch of Oph-5 with a higher ratio of 7Me to 6Me species was used in this experiment (see Fig. S5 for a comparison between the batches). **(e, f)** EICs of the 7-fold **(e)** and 6-fold **(f)** methylated substrates and respective cyclic products over the time course (z-axis). The relative abundance is set to 100 for the respective substrate at each time point.

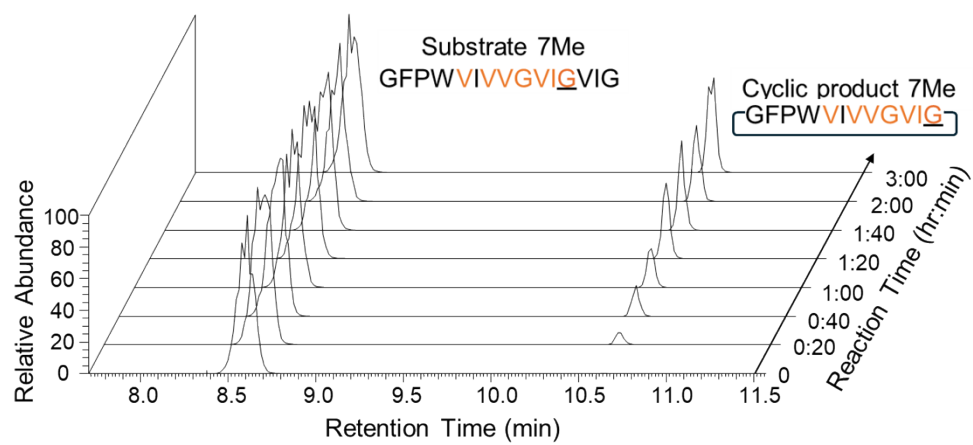
a



b**Product formation at equimolar (90 μ M) substrate concentration**

c**d**

e



f

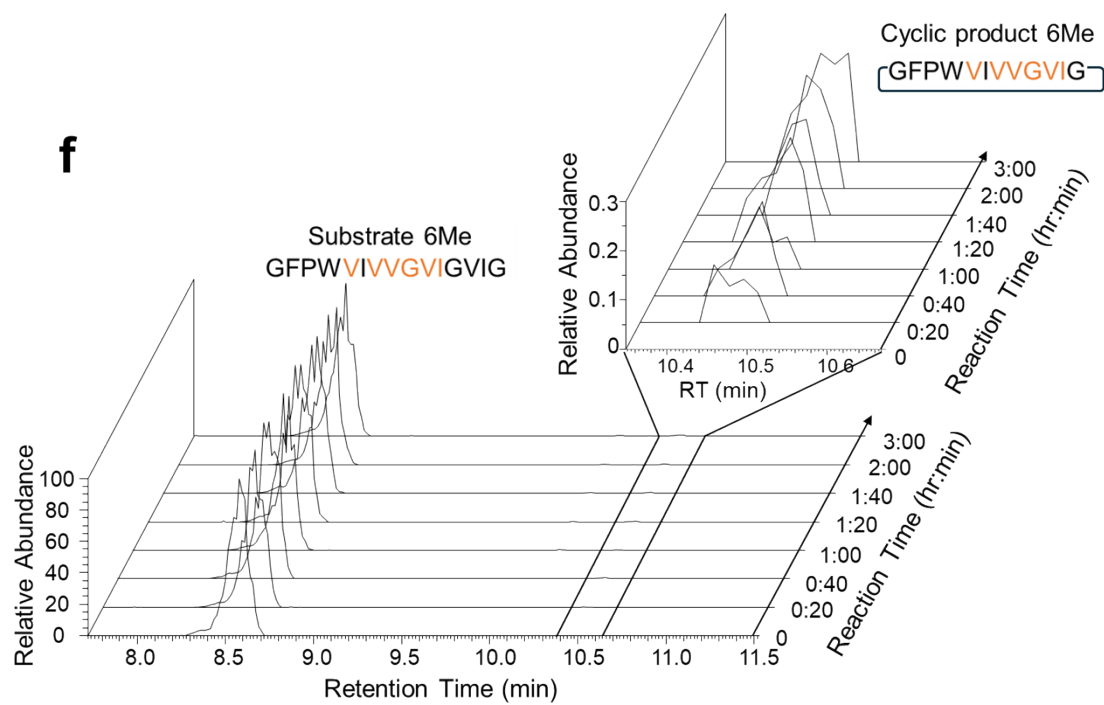


Figure S13. Activities of GmPOPB and OphP towards synthetic peptides PHA1 and AMA1. Peptides PHA1 and AMA1 are known to be processed by GmPOPB protease^[1,5]. The graphs show the HPLC-UV-VIS chromatograms with optical density (OD) at 280nm. The synthetic peptides were stored at 1 mg/ml in phosphate buffer at pH 6.0. For the reaction, 20 μ M substrate was used with 1 μ M of OphP or GmPOPB in the standard assay buffer [50 mM HEPES pH 6.0 + 10 mM DTT]. The reaction mixture (50 μ l) was incubated at 30°C, 600 rpm, overnight. The reaction was quenched by the addition of 50 μ l methanol. After centrifugation at the highest speed at 4°C, 5 μ l supernatant was used for HPLC-MS/MS analysis. No cyclic peptides were observed for PHA1 in the UV trace due to low abundance. The peak around 12 min, marked with an asterisk, is unspecific as it does not correspond to any product. The amanitin and phallacidin core peptides are underlined. The products are indicated by a blue arrow.

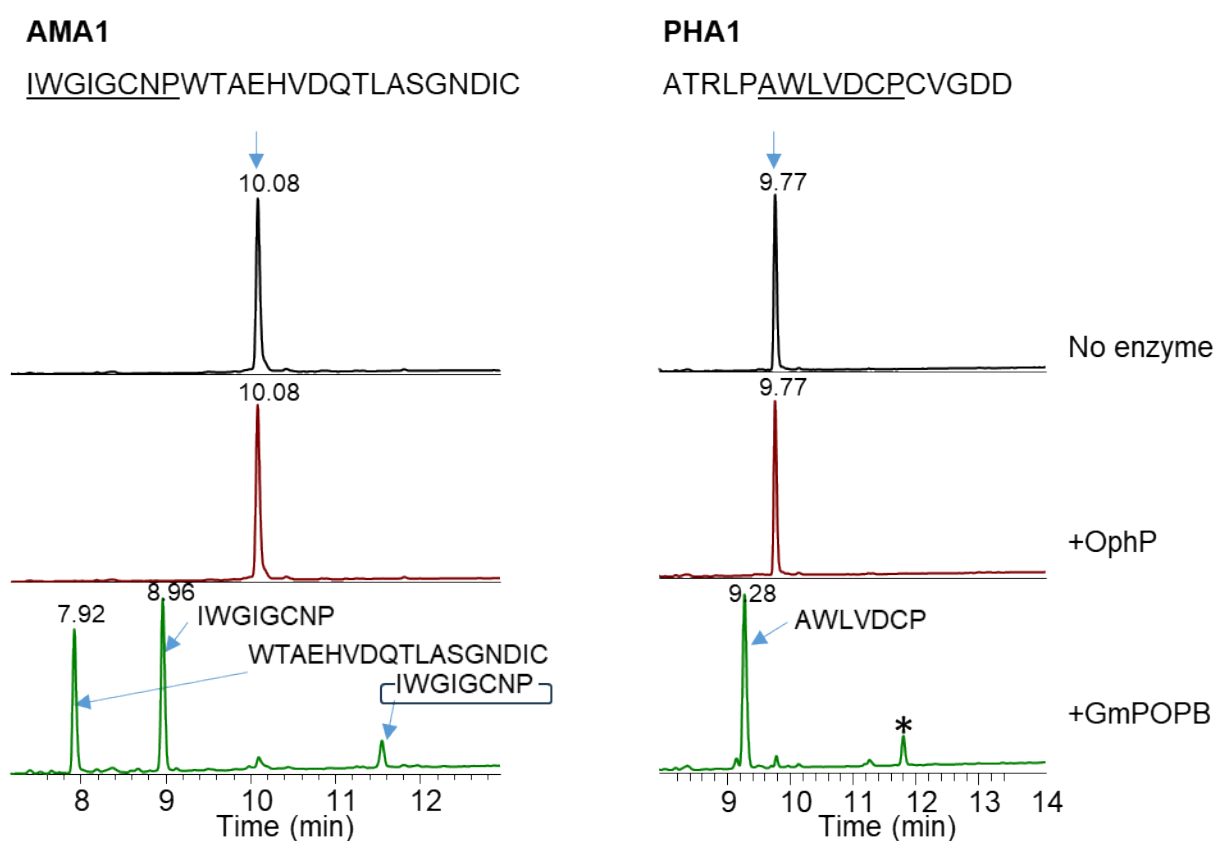
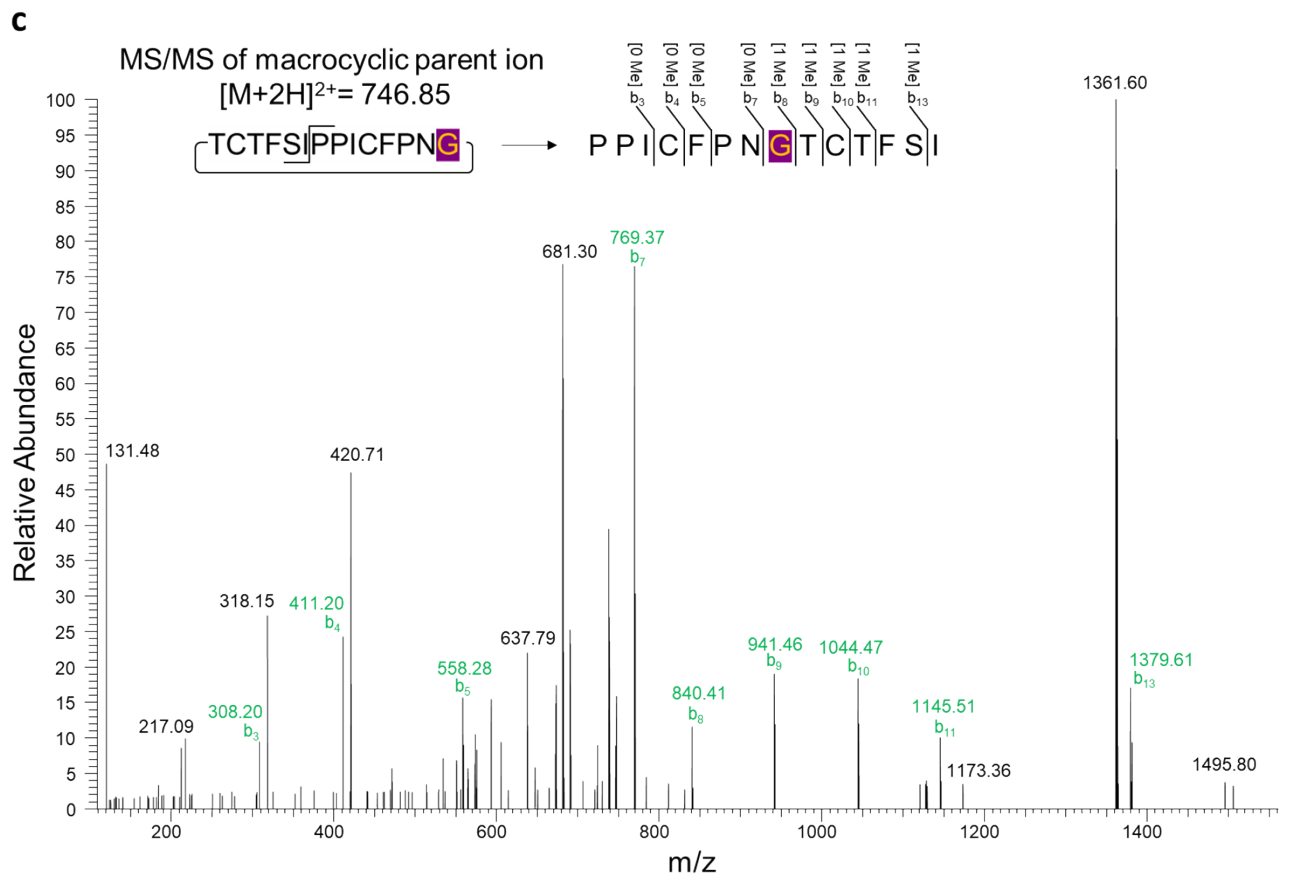
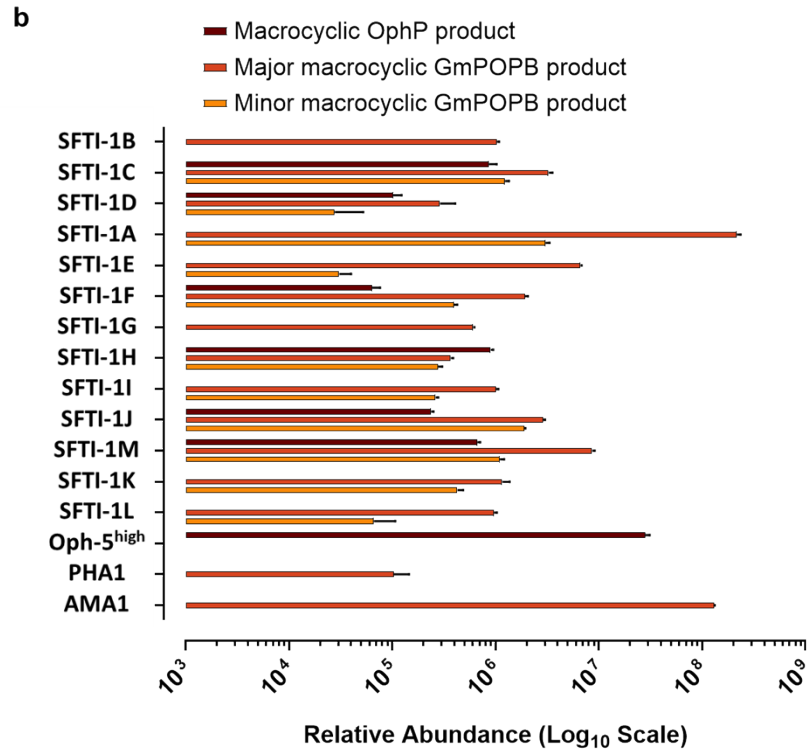


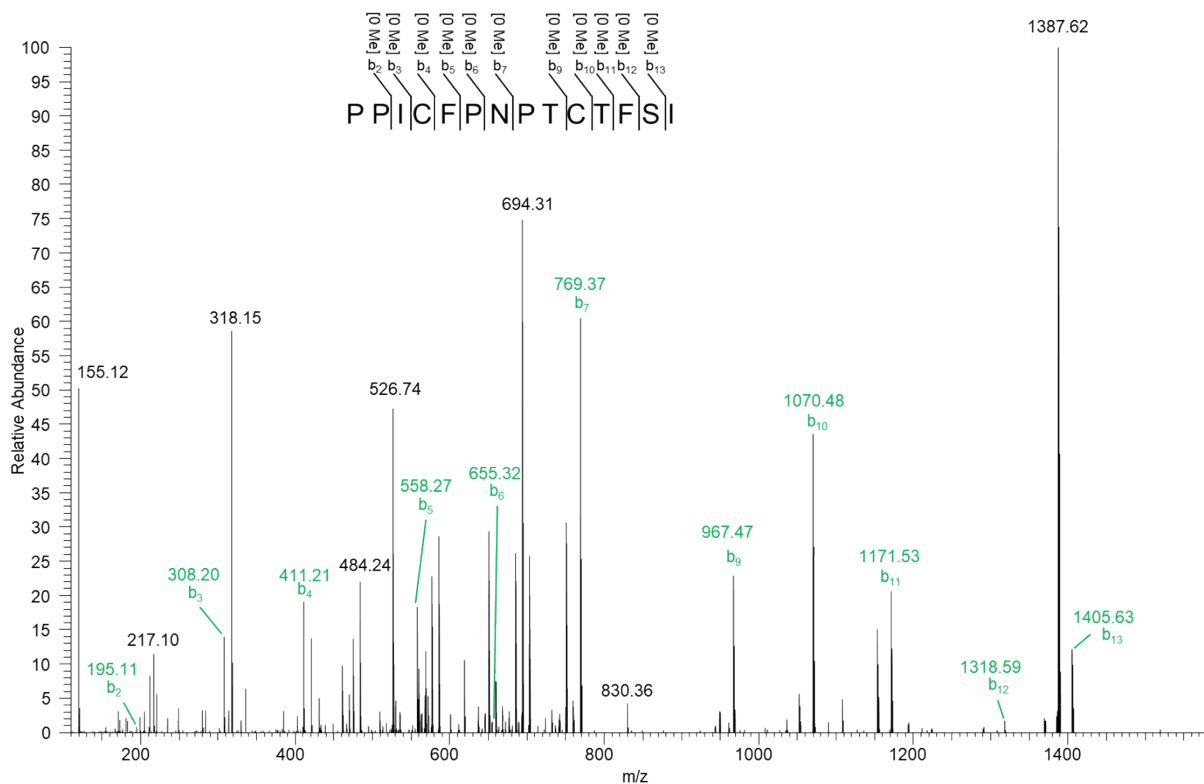
Figure S14. Overview, relative abundance and LC-MS/MS spectra of macrocyclic peptide products. Macrocyclic products obtained from incubation of OphP or GmPOPB with synthetic SFTI-1 variant peptides. **(a,b)** Overview and relative abundance of the obtained macrocyclic peptides. **(c-k)** LC-MS/MS with b-ions and y-ions in green are shown for one of the possible permutations for ring opening of the macrocyclic peptide. Mass tolerance between observed masses and the theoretical masses was set at 10 ppm. Mass precision was set at 4 decimals, but m/z values are rounded to two decimals in the figures. **(c)** cyclic TCTFSIPPICFPN^{me}G **(d)** cyclic TCTFSIPPICFPNP **(e)** cyclic TCTFSIPPICFPN^{me}A **(f)** cyclic TCTFSIPP **(g)** cyclic NGTCTFSIPPICFP **(h)** cyclic NGTCTFSIPP **(i)** cyclic TCTF^{me}SIPPICFPN^{me}G **(j)** cyclic TCTF^{me}SIPPICFP **(k)** cyclic TCTFSIPPICFP **(l)** cyclic ATRLPAWLVDGP **(m)** cyclic IWGIGCNPP **(n)** EIC peak area of SFTI-1A substrate and cyclic product NGTCTFSIPPICFP after incubation with or without GmPOPB

a

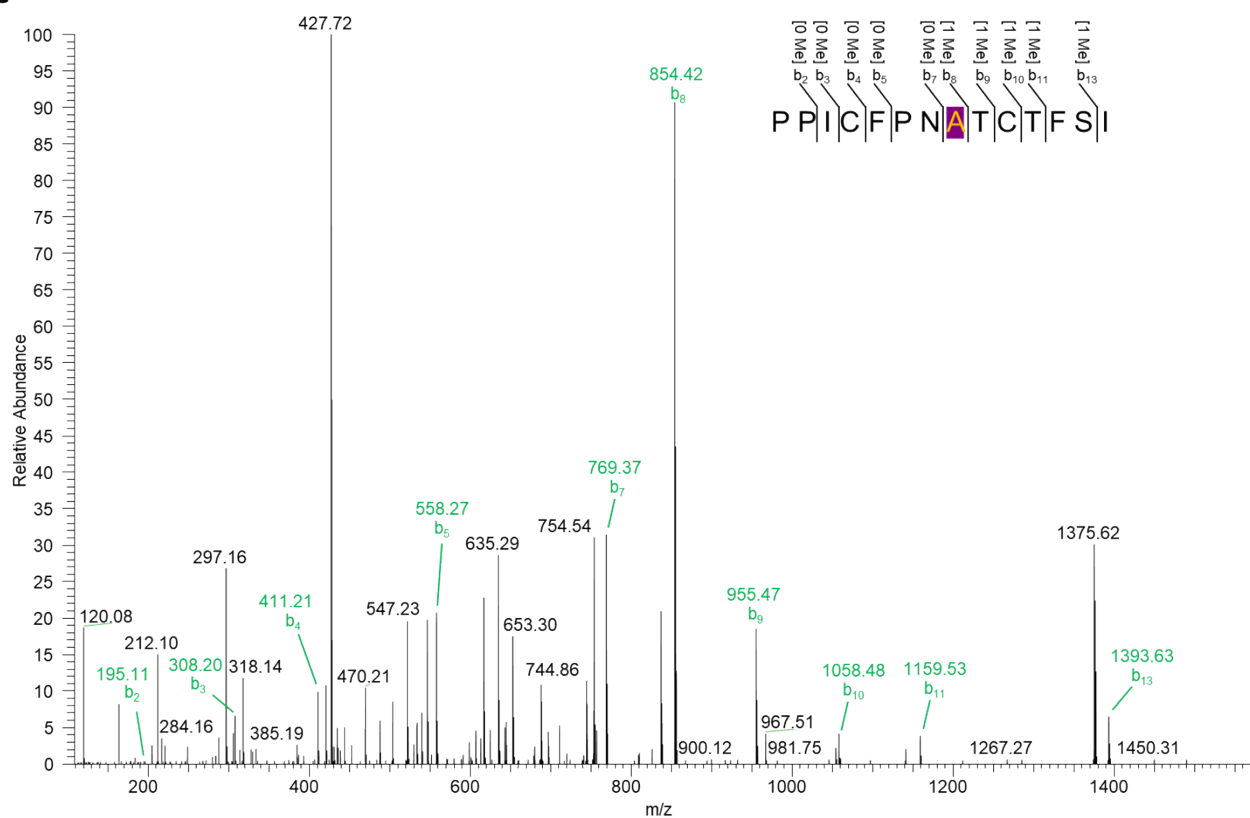
Peptide Substrate Name	Peptide substrate Sequence	Macrocyclic OphP product	Major macrocyclic GmPOPB product	Minor macrocyclic GmPOPB product
SFTI-1B	TCTFSIPPICFPNGSVMSTE	None	[TCTFSIPP]	None
SFTI-1C	TCTFSIPPICFPN ^G SVMSTE	[TCTFSIPPICFPN ^G]	[TCTFSIPP]	[TCTFSIPPICFPN ^G]
SFTI-1D	TCTFSIPPICFPN ^G SVMSTE	[TCTFSIPPICFPN ^G]	[TCTFSIPPICFPN ^G]	[TCTFSIPPICFP]
SFTI-1A	NGTCTFSIPPICFPWTAEHVDQTLASGNDIC	None	[NGTCTFSIPPICFP]	[NGTCTFSIPP]
SFTI-1E	TCTFSIPPICFPNGASGNDI	None	[TCTFSIPP]	[TCTFSIPPICFP]
SFTI-1F	TCTFSIPPICFPN ^G ASGNDI	[TCTFSIPPICFPN ^G]	[TCTFSIPP]	[TCTFSIPPICFPN ^G]
SFTI-1G	TCTFSIPPICFPNGSIGNDA	None	[TCTFSIPP]	None
SFTI-1H	TCTFSIPPICFPN ^G SIGNDA	[TCTFSIPPICFPN ^G]	[TCTFSIPPICFPN ^G]	[TCTFSIPP]
SFTI-1I	TCTFSIPPICFPNASIGNDA	None	[TCTFSIPP]	[TCTFSIPPICFP]
SFTI-1J	TCTFSIPPICFPN ^A SIGNDA	[TCTFSIPPICFPN ^A]	[TCTFSIPPICFPN ^A]	[TCTFSIPP]
SFTI-1M	TCTFSIPPICFPN ^E SIGNDA	[TCTFSIPPICFPN ^E]	[TCTFSIPPICFPN ^E]	[TCTFSIPP]
SFTI-1K	TCTFSIPPICFPN ^V SIGNDA	None	[TCTFSIPP]	[TCTFSIPPICFP]
SFTI-1L	TCTFSIPPICFPN ^V SIGNDA	None	[TCTFSIPP]	[TCTFSIPPICFP]
Oph-5 ^{high}	GFPWVIVGVIGVIG	[GFPWVIVGVIG]	None	None
PHA1	ATRLPAWLVDCECVGDD	None	[ATRLPAWLVDCE]	None
AMA1	IWGIGCN ^E WTAEHVDQTLASGNDIC	None	[IWGIGCN ^E]	None



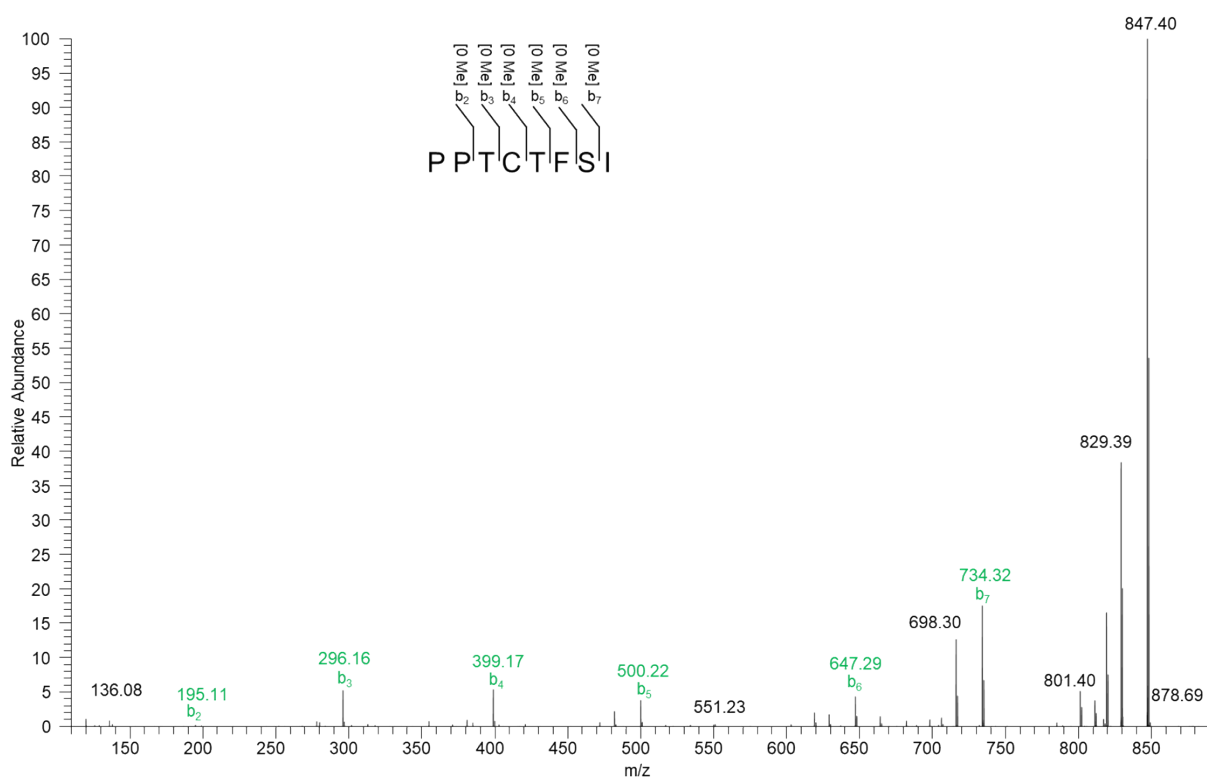
d



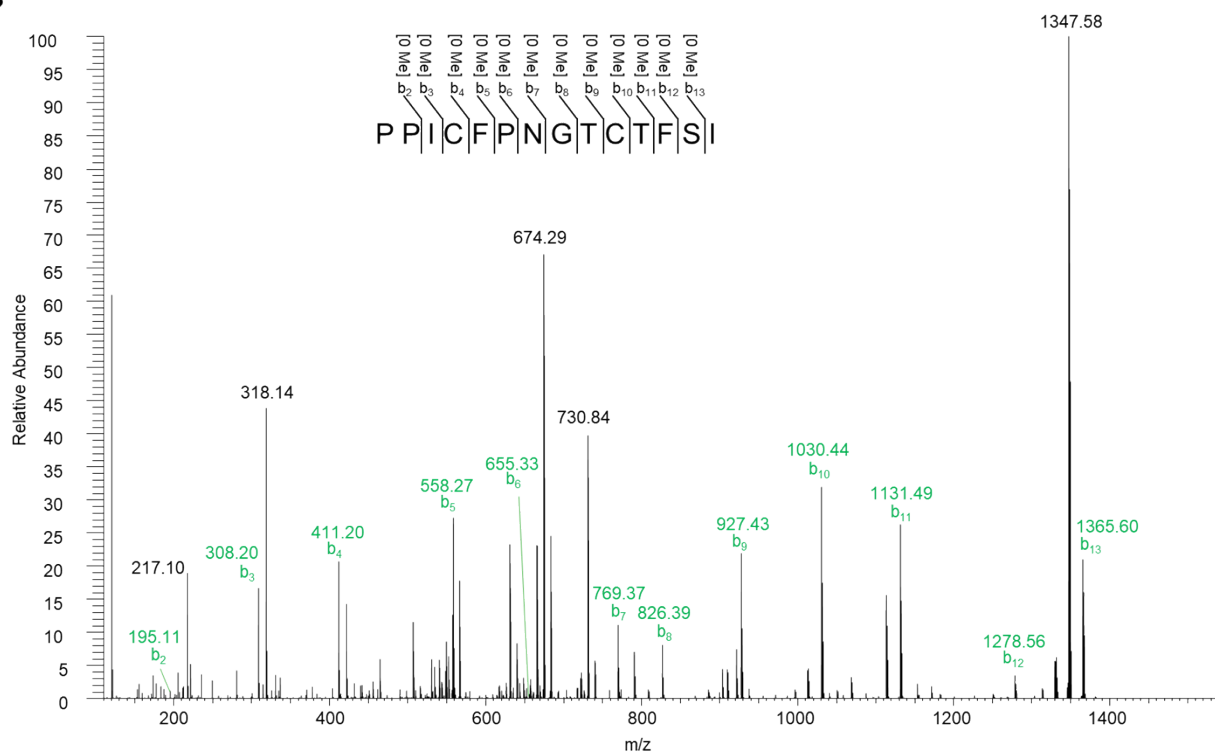
e



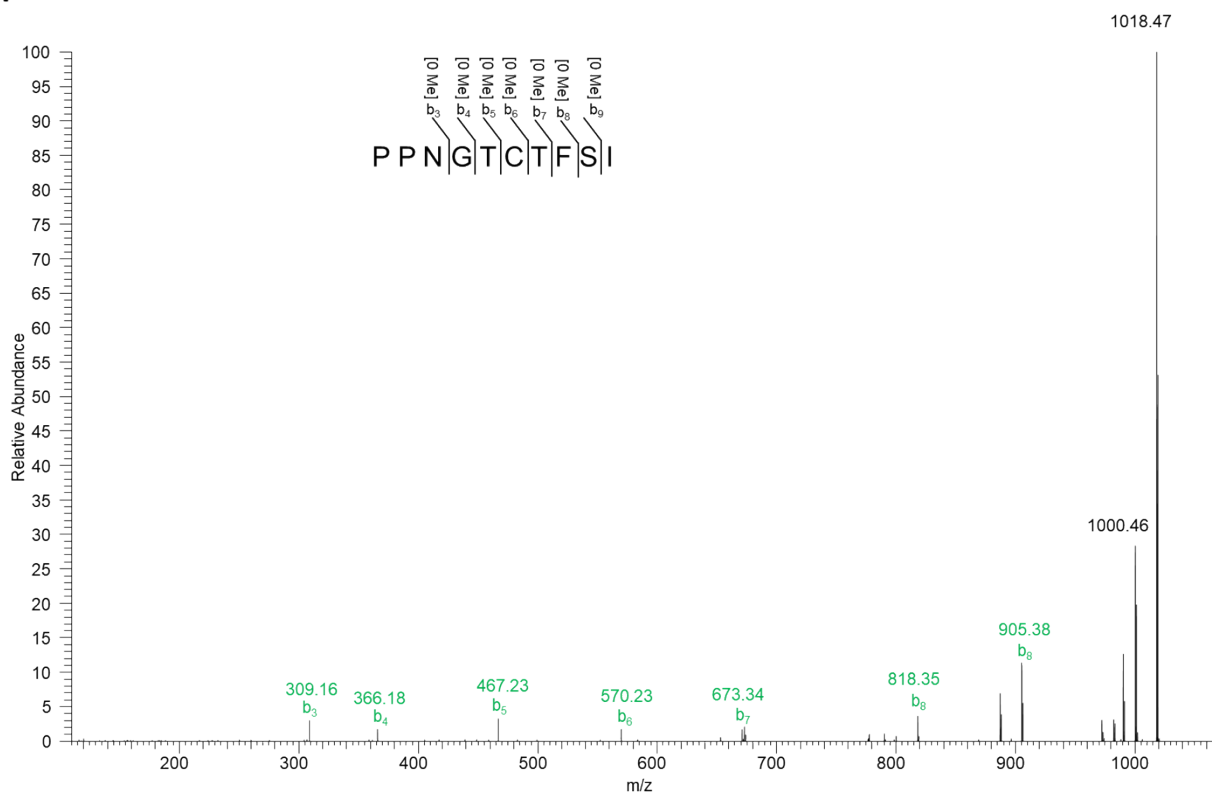
f



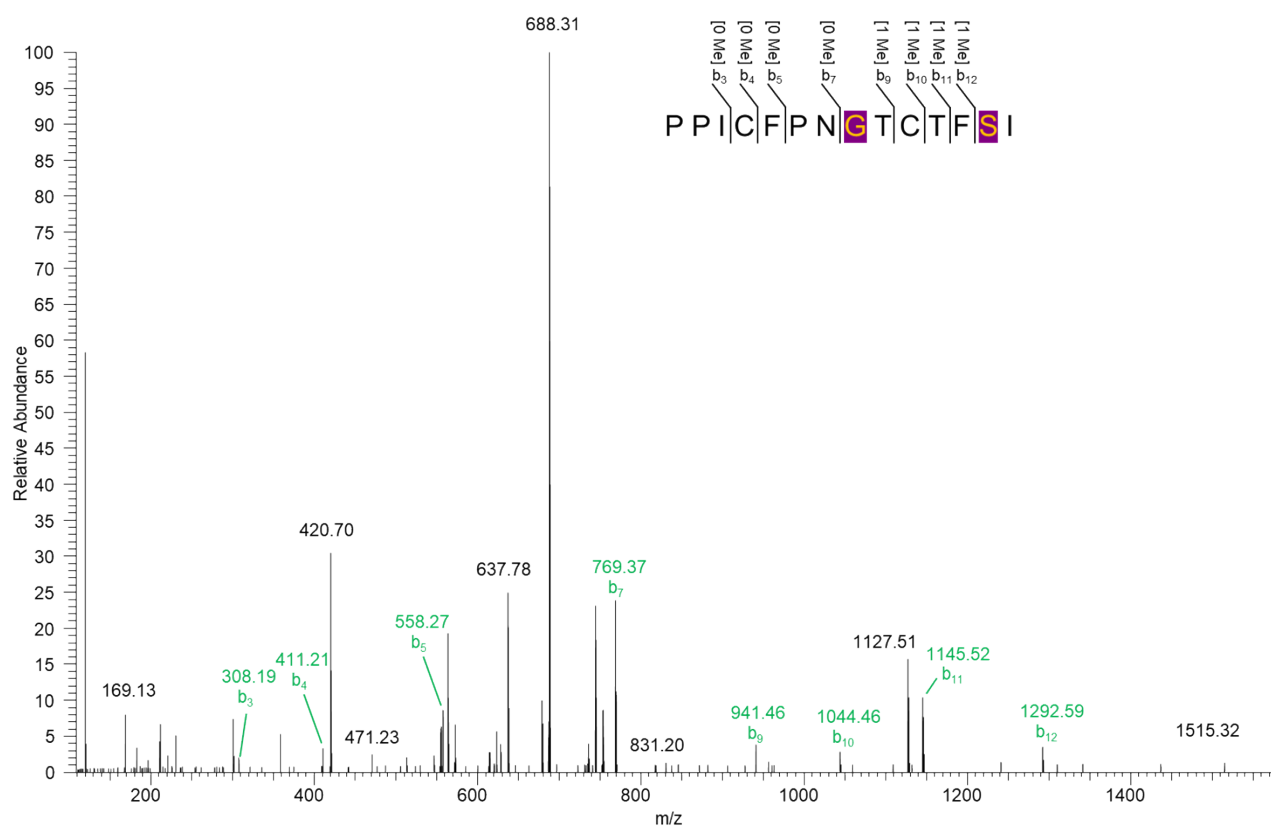
g



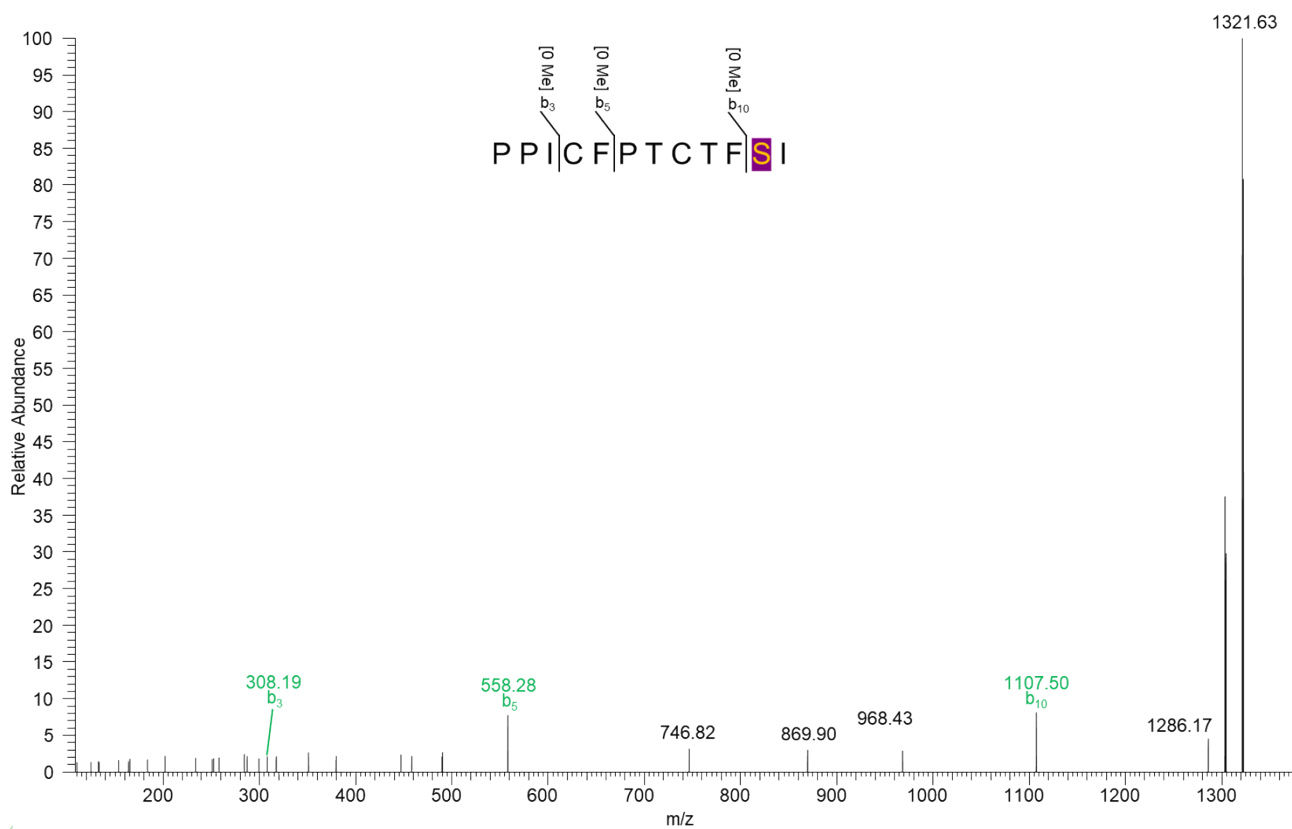
h



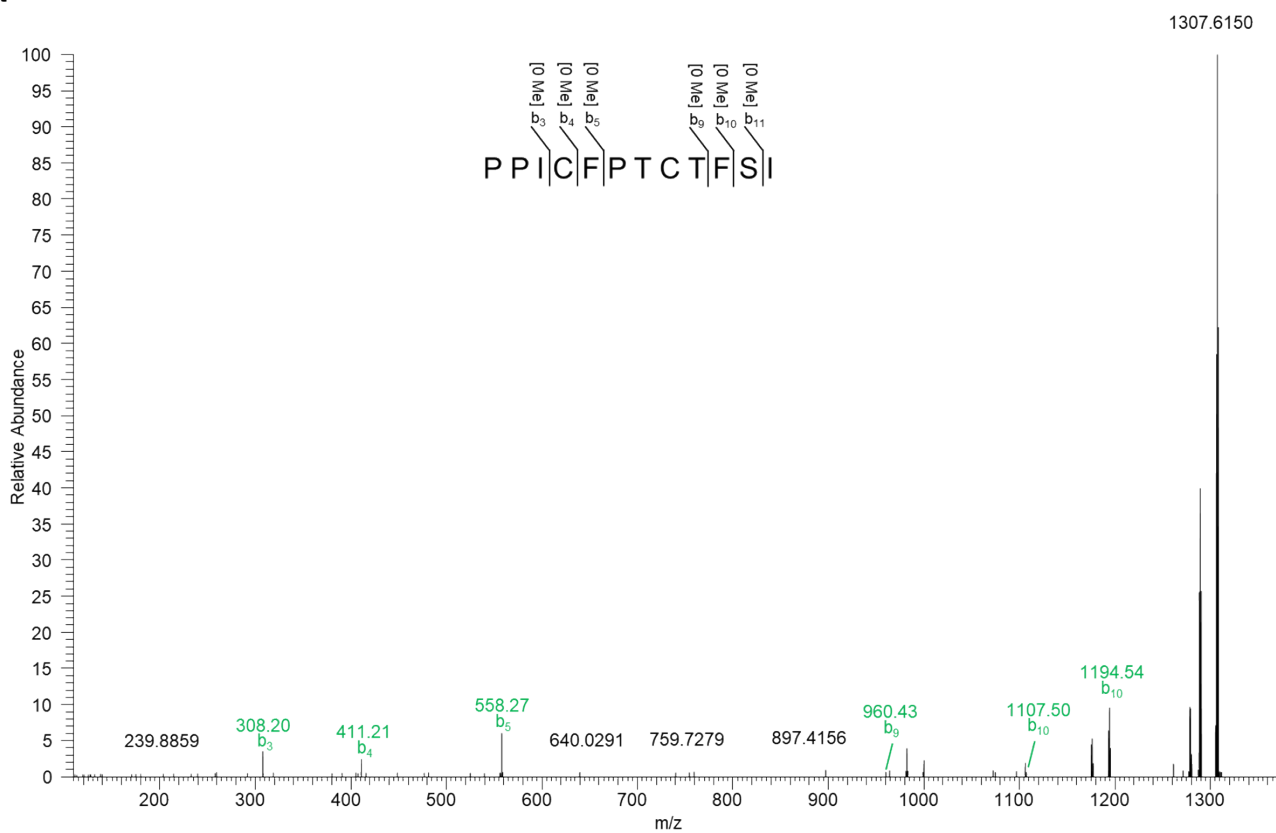
i



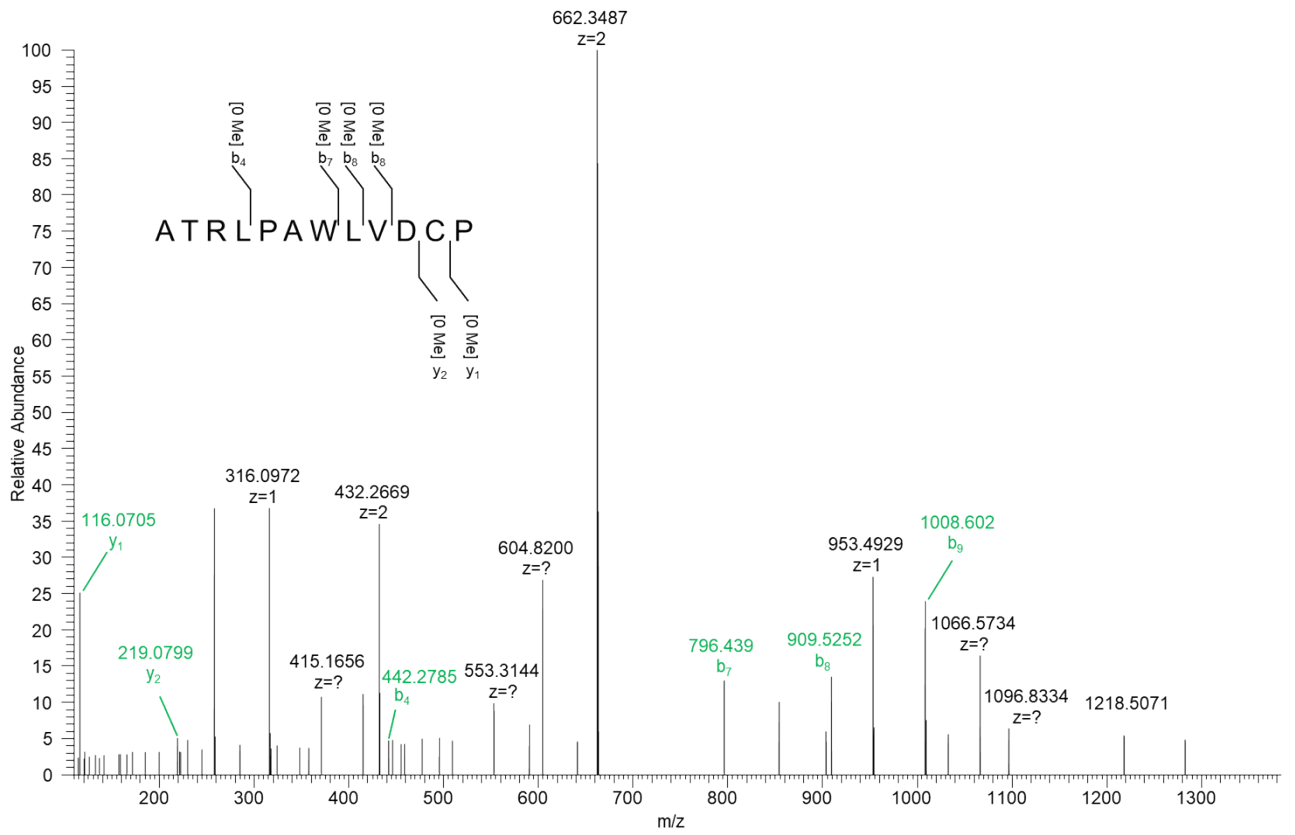
j



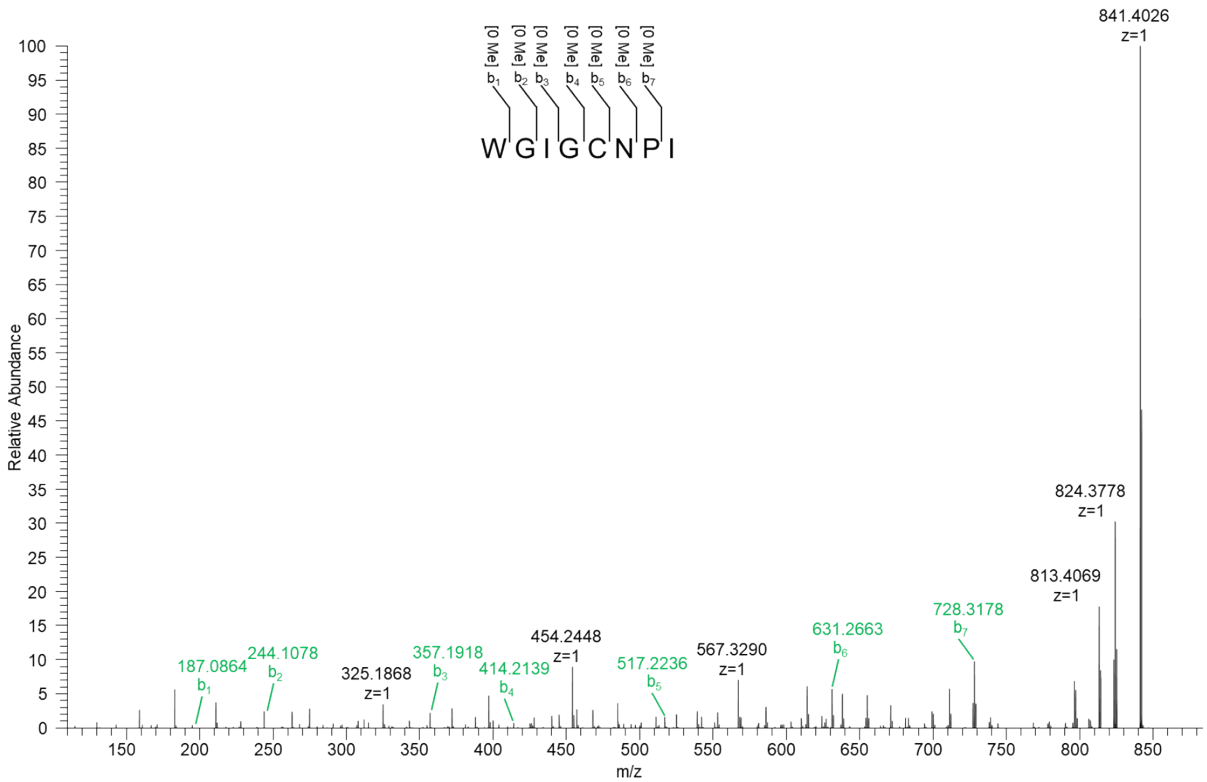
k



I



m



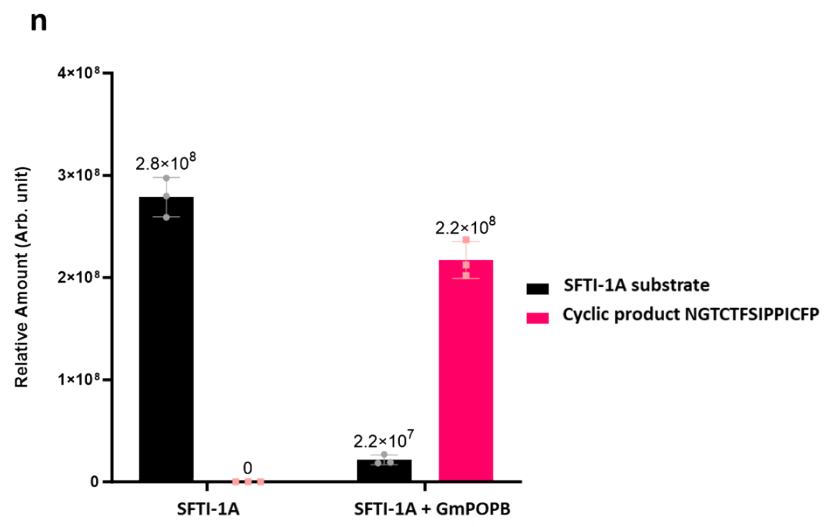


Figure S15. Cartoon and electrostatic surfaces of apo OphP (PDB 7ZB2), apo GmPOPB (PDB 5N4F) and apo human dipeptidyl peptidase IV (DPP-IV, PDB 1NU6). The view through the β -propeller and side views of (a) apo OphP with the Oph-6 substrate (yellow spheres), (b) apo GmPOPB with the 35mer substrate (yellow spheres), and (c) apo DPP-IV with modelled tripeptide substrate (yellow spheres). Electrostatic calculation was performed using the APBS-PDB2PQR software suite under the default setting and drawn in PyMol. The electrostatic

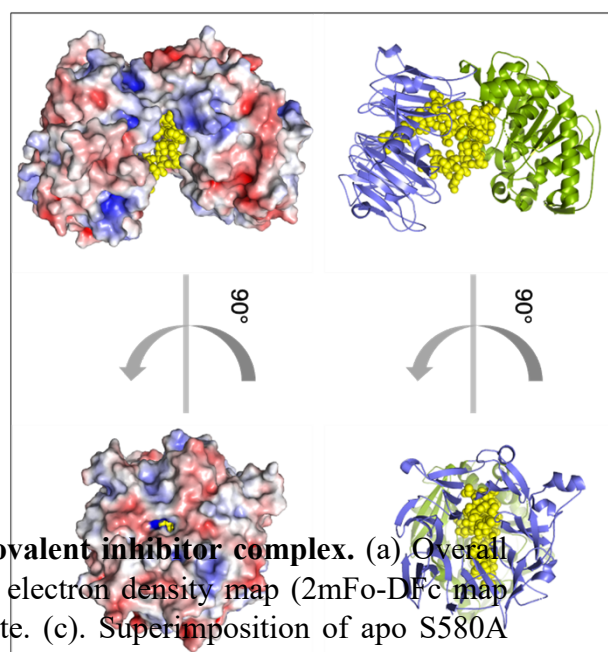
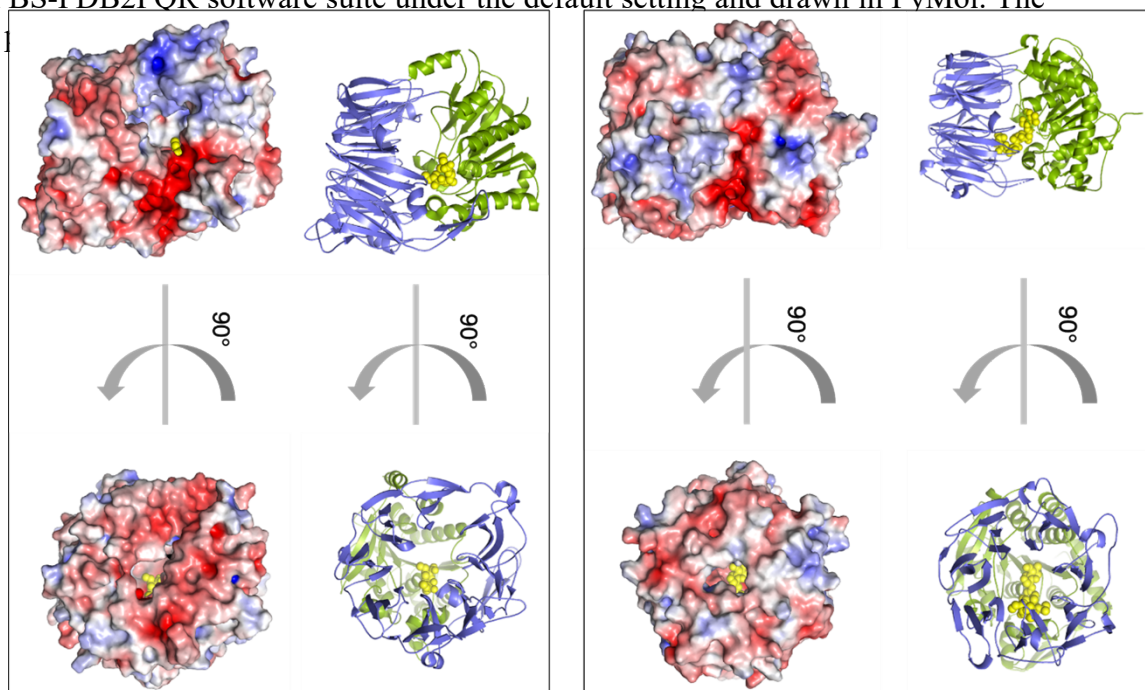


Figure S16. Crystal structure of the OphP:ZPP covalent inhibitor complex. (a) Overall structure of the OphP:ZPP complex (b) σ_A -weighted electron density map ($2mFo-DFc$ map contoured at 1σ) showing the S580-acyl intermediate. (c). Superimposition of apo S580A (subunit A green and H grey, both have ordered loop region Leu697-Thr707) with OphP:ZPP complex (subunit A colored in salmon). The black arrows illustrate the large movement of two loops (Ser164-Met171, and Leu697-Thr707) when ZPP is bound. As a result of the 7.6 Å shift of His701 it is now part of the catalytic triad in the OphP:ZPP complex. The movement of Asp156 upon ZPP results in a salt bridge and Arg667 in the OphP:ZPP complex.

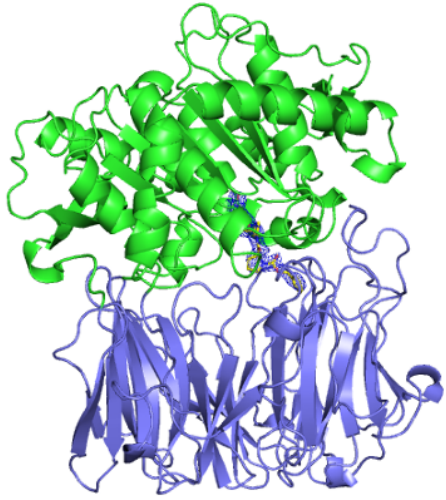
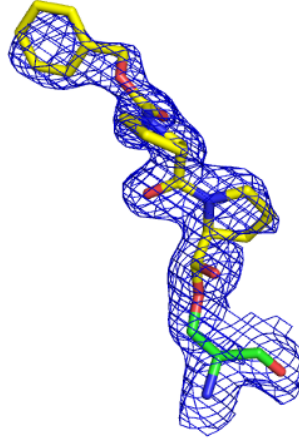
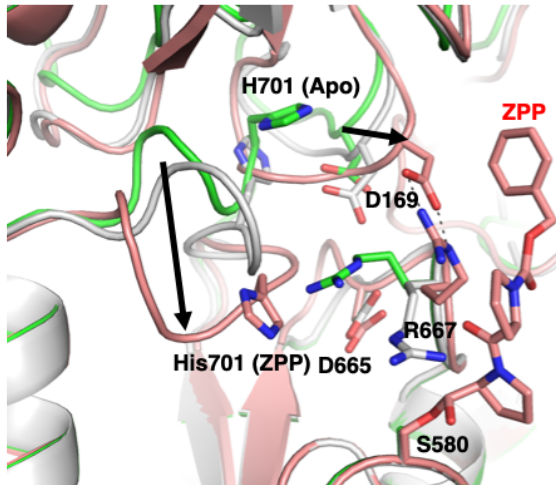
a**b****c**

Figure S17. Multiple sequence alignment of OphP with post-proline cleaving prolyl oligopeptidases (POPs). The sequence of OphP is used as a query and blasted (protein-protein BLAST) against the UniProtKB/SwissProt database. Sequences are further selected by removing all the dipeptidyl peptidase family enzyme sequences. Multiple sequence alignment was created with MUSCLE¹⁵ and rendered as white and black with ESPrpt 3.0¹⁶. The hydrophobic pocket residues accommodating P1 proline are highlighted by underlying solid red triangles and catalytic triad residues are shown in solid purple triangles. Secondary structure elements of OphP are depicted above the aligned sequence. Black box with white character shows strict identity, bold black character similarity, and black frame similarity across groups. Names, UniProt ID and corresponding organisms are as follows: PCY1, R4P353, *Gypsophila vaccaria*; GmPOPB, H2E7Q8, *Galerina marginata*; GmPOPA, H2E7Q7, *Galerina marginata*; AbPOPB, E2JFG2, *Amanita bisporigera*; AbPOPA, E2JFG1, *Amanita bisporigera*; PfuPOP, Q51714 (PDB entry 5T88), *Pyrococcus furiosus*; AhPOP, Q06903, *Aeromonas hydrophila*; EmPOP1, P27028, *Elizabethkingia meningoseptica*; EmPOP2, P27195, *Elizabethkingia meningoseptica*; DbPOP, Q86AS5, *Dictyostelium discoideum*; MmPOP, Q9QUR6, *Mus musculus*; P48147, *Homo sapiens*; BtPOP, Q9XTA2, *Bos taurus*; SsPOP, P23687 (PDB entry 1QFS), *Sus scrofa*. Sequence of DbiP from *Dendrothele bisporea* is retrieved from Joint Genome Institute website (name: gm1.24165_g, protein ID: 871165, location: scaffold_621:21283-24607). The sequence of LedP from *Lentinula edodes* is obtained from NCBI database (GAW09065).

OphP TT α3 β35 TT α4 η8 α5 TT β36

500 510 520 530 540 550 560 570 580

OphP GGFSLAMLP TFSLS TLL FCKIYRAIYATNIRGGSEYGESWHREGMLDKKQNVFDDFNAAETEWLIANKYASKDRIATRGGSNGGVL
LedP GGFSLAMLP TFSVSTLL FCKIYRAMYVVENIRGGSEFGESWHREGMLDKKQNVFDDFNAAETKWLVA NKYANKYNVAIRGGSNGGVL
DbiP GGFSLAMLP TFSVSTLL FCKIYRAI... GGSEYGESWHRAGMLGNKQNVFDDFNAAETEWLVANKYANKD RVAIRGGSNGGVL
PCY1 GGFSLMMPTFSASRI VFLKHLGGVFC LANIRGGSEYGE EWHKAGFRD KQNVFDDFI SAAEYLISSGYTKARRVAIRGGSNGGVL
GmPOPB GGFATISADPF FSPFIILT FLQTYGAIFAVPSIRGGSEFGEEWHKGRRET KVNTFDDFI AAAQFLVKNKYAAPGKVAINGASNGGVL
AbPOPB GGFATISADPF FSPFIILT FMQTYGAILAVENIRGGSEFGGEWHKGRRET KVNTFDDFI AAAQFLVKNKYAAPGKVAITGASNGGVL
GmPOPA GGFATISIDPF FFSATILT FLQKYGVVFALFNIRGGSEFGEDWHLACREKKGNCFDDFI AATQYLVKNKYAAPDKVTIINGGSNGGVL
AbPOPA GGFATISINPF FFSPTILT FLQKYGA I LAVENIRGGSEFGETWHDAGIRREK RANVYDDFI AATQFLVKNKYAAPGKVAINGGSNGGVL
PfuPOP GGFNIALTPMFFPQVIFPFLKR... GGTFIMANLRGGSEYGE EWHRAGMRENKQNVFDDFI AVLEK LKKEGY... KVAAGRSGNGGVL
AhPOP GGFVSLTTPSF SVSVANWLDL... GGVIYAVANLRGGSEYGOAWHLA GTRMNKQNVFDDFI AAEEYLKKEGYTRTRDLAIRGGSNGGVL
EmPOP1 GGFNISLOPAF SVVNAIWMEN... GGIYAVPNIRGGSEY GK KWH D AGTKMQKKNVFNDFI AAGEYLQKNGYTSKEYMALSGRSGNGGVL
EmPOP2 GGFNISLOPAF SVVNAIWMEN... GGIYAVPNIRGGSEY GK KWH D AGTKMQKKNVFNDFI AAGEYLQKNGYTSKDYMALSGRSGNGGVL
DbPOP GGFNISYITQSF SIRNLYFLNKFNGIFVIANIRGGSEY GKAWHEAGSKKNKQNVFDDFI GAEEYLKIKENYTNQNKLAIRGGSNGGVL
RnPOP GGFNISITPNYSVSR LIFVRHMGVVLAVANIRGGSEYGETWHKGGILANKQNVFDDFI QCAAEYLKKEGYTTSKRLTINSGSNGGVL
MmPOP GGFNISITPNYSVSR LIFVRHMGVVLAVANIRGGSEYGETWHKGGILANKQNVFDDFI QCAAEYLKKEGYTTSKRLTINSGSNGGVL
HsPOP GGFNISITPNYSVSR LIFVRHMGVVLAVANIRGGSEYGETWHKGGILANKQNVFDDFI QCAAEYLKKEGYTTSKRLTINSGSNGGVL
BtPOP GGFNISITPNYSVSR LIFVRHMGVVLAVANIRGGSEYGETWHKGGILANKQNVFDDFI QCAAEYLKKEGYTTSKRLTINSGSNGGVL
SsPOP GGFNISITPNYSVSR LIFVRHMGVVLAVANIRGGSEYGETWHKGGILANKQNVFDDFI QCAAEYLKKEGYTTSKRLTINSGSNGGVL

F502

S580 N581

OphP α6 η9 β37 η10 η11 α7 α8 η12 T...T β38

590 600 610 620 630 640 650 660

OphP TTAACANQAP... GLYRCVITIEGIIDMLRFPKFTFGALWSEYGDPEDEPED... FDFIFKYSPPVHNIP... PPG... DTVMPAMLFFTTAA
LedP TTAACANQAP... GLYRCVITIGGIIDMLRFPKFTFGALWSEYGDPEDEPED... FDFIYKYSPPVHNIP... PSG... DVVLPAMLFFTTAA
DbiP TTAACANQAP... GLYRCVITIGGIIDMLRFPKFTFGALWSEYGDPEDEPEA... FDFIYKYSPPVHNIP... PSG... ETVMPAMLFFTTAA
PCY1 VAAACINQRP... DLFGCAEANC GVM DMLRFPKFTFLGLWTGDYCSDEKEE... FKWLIKYSPIHNVRREWEQPGNEETQYPATMILTNI
GmPOPB VMGSIVRAPEGT FGAAVPEG GVA D L L K F H K F T G G A W I S E Y G N S I P E E ... F D Y I Y P L S P V H N V ... R T ... D K V M P A T L I T V N I
AbPOPB VCGSVVRAPEGT FGAAVSEG GVA D L L K F H K F T G G A W I S E Y G N P F I K E D ... F D F V Q A L S P V H N V ... P K ... D R V L P A T L L M T N A
GmPOPA VSA CVNRAP EGT FGCAVADV GVH D L L K F H K F T I G K A W T S D Y G N P D D P N D ... F D F I F P I S P L Q N I ... P K ... D K V F P M L L T A D
AbPOPA VAA CVNRAREGT FGAAIAEV GV D L L K F H K F T I G K A W I S D Y G D P E D P R D ... F D Y I Y T H S P L H N I ... P K ... N M V L P P T M L L T A D
PfuPOP VSA I L T Q R P ... D V M D S A L I G Y P V I D M L R F H K L Y I G S V W I P E Y G N P E D P K D ... R E F L L K Y S P V H N V ... D P K ... K K Y P P L I Y T G L
AhPOP VGA I T M T R P ... D L A K V A F P G V G V D M L R Y N K F T A G A G W A Y D Y G T A E D S K E M F E Y L K S Y S P V H N V ... K A G ... T C Y P S T M V I T S D
EmPOP1 VGA I T M T R P ... D L A K V A F P G V G V D M L R Y N K F T A G A G W A Y D Y G T A E D S K E M F E Y L K S Y S P V H N V ... K A G ... T C Y P S T M V I T S D
EmPOP2 VGA I T M T R P ... D L A K V A F P G V G V D M L R Y N K F T A G A G W A Y D Y G T A E D S K E M F E Y L K S Y S P V H N V ... K A G ... T C Y P S T M V I T S D
DbPOP MGA I S N Q R P ... D L F K C V V A D V G V M D M L R F H L T T I G N W V S D Y G R S D N P Q D ... F D V L I K Y S P L N N V ... P K ... D S N Q Y P S I M L C T G D
RnPOP VAA CANQRP... DLFGCVIAQV GVM DMLK F H K F T I G A W T T D Y G C S D S K Q H ... F E W L L K Y S P L H N V K ... L P E A D D I Q Y P S M L L L T A D
MmPOP VAA CANQRP... DLFGCVIAQV GVM DMLK F H K F T I G A W T T D Y G C S D S K Q H ... F E W L L K Y S P L H N V K ... L P E A D D I Q Y P S M L L L T A D
HsPOP VAA CANQRP... DLFGCVIAQV GVM DMLK F H K Y T I G A W T T D Y G C S D S K Q H ... F E W L V K Y S P L H N V K ... L P E A D D I Q Y P S M L L L T A D
BtPOP V A T C A N Q R P ... D L F G C V I A Q V G V M D M L K F H K Y T I G A W T T D Y G C S D S K Q H ... F E W L I K Y S P L H N V K ... L P E A D D I Q Y P S M L L L T A D
SsPOP V A T C A N Q R P ... D L F G C V I A Q V G V M D M L K F H K Y T I G A W T T D Y G C S D S K Q H ... F E W L I K Y S P L H N V K ... L P E A D D I Q Y P S M L L L T A D

I606

W621 Y625

OphP α9 β39 α10

670 680 690 700 710 720 730 740

OphP YDDRVSPLHTEKHVAALQHNF... GPNPCLMRIDLN... SGHFACKSTQEMLEETADEYSFIGKSMGLTMTQTQGSVDSSRWSC
LedP YDDRVSPLHTEKHVAALQYNFP... GPNPCLMRIDLN... TGHFACKSTQKMLEETADEYSFIGKSMGLVMCAQNEHASKQWSC
DbiP YDDRVSPLHTEKHVAALQHNSFP... GPNPILMRVDMN... SGHYACKSTQKMLEETADEYSFIGKSMGLTMTQVENKSDSNRWSC
PCY1 HDDRVPVPLHSEKLLATMQHVLCTSLSDSPQKNPIARIQRK... AAHY... GRATMTQIAEVADR YGFMAKALEAPWID...
GmPOPB GDDRVPVPMHSEKFIATLQHNVPQ... NPHPLLIKIDKSWLGHGMGKPTDKNVKDAADK WGFIA RALGLLEKTVE...
AbPOPB GDDRVPVPMHSLKFVANLQYNVPQ... NPHPLLIRVDKSWLGHGFGKTTDKHTKDAADKWSFVAQSLGLEWKTVD...
GmPOPA HDDRVPVPMHSEKLAALQYSLPH... NPNPLLIRIDKK... AGHGACKSTQQKIKESADK WGFVAQSLGLVWKDSTEQPNL...
AbPOPA HDDRVPVPMHSEKYYAAMLYTTLPH... NRHP L L L R V D K K ... A G H G G K S T E K R L O E A A D K W G F A A Q S M G L A W K D R Q A N L ...
PfuPOP HDDRVPVPAHALKFFMKLKE... IGAPVYLRVETK... SGH... MCA SPETRARELTDLLAFV LK T L S ...
AhPOP HDDRVPVPAHSEKFAATLQADDA... GPHPQLIRIETN... AGHGACTPVAKLIEQSADIIYAFTLFEMGYRQLPRQP...
EmPOP1 HDDRVPVPAHSEKFGSELQAKQS... CKNPILIRIETN... AGHGAGRSTEQVVAENADLLSFALYEMG I K S L K ...
EmPOP2 HDDRVPVPAHSEKFGAELQAKQA... CKNPVILIRIETN... AGHGAGRSTEQVVMENADLLSFALYEMG I K N L K ...
DbPOP HDDRVPVPAHSEKFGSELQYQLGKK... VDTPLLIRVDK... SGHGAGKGLSKQNNIADIENFFSKVLNVKLNLF...
RnPOP HDDRVPVPLHSLKFIATLQYIVGRSRK... QSNP L L I H V D T K ... A G H G B G K P T A K V I E E V S D M F A F I A R C L N I E W I Q ...
MmPOP HDDRVPVPLHSLKFIATLQYIVGRSRK... QSNP L L I H V D T K ... A G H G A K P T A K V I E E V S D M F A F I A R C L N I E W I Q ...
HsPOP HDDRVPVPLHSLKFIATLQYIVGRSRK... QSNP L L I H V D T K ... A G H G A K P T A K V I E E V S D M F A F I A R C L N I D W I P ...
BtPOP HDDRVPVPLHSLKFIATLQHLVGRSRK... QNNP L L I H V D T K ... A G H G A K P T A K V I E E V S D M F A F I A R C L N I D W I P ...
SsPOP HDDRVPVPLHSLKFIATLQYIVGRSRK... QNNP L L I H V D T K ... A G H G A K P T A K V I E E V S D M F A F I A R C L N I D W I P ...

D665 V668

H701

Figure S18. Surface of the P1 pocket of GmPOPB (PDB 5N4C), PCY1 (PDB 5UW6) and OphP (PDB 7ZAZ and 7ZB1) (all white) accommodating the covalent serine acyl intermediate of ZPP (yellow). (a,b) The canonical P1 pockets of GmPOPB and PCY1 can accommodate proline well at the cleavage P1 site. (c,d) Accommodation of the proline residue of ZPP in OphP (PDB 7ZAZ) requires conformational change of Ile606 compared to OphP-Oph-6 (PDB 7ZB1). In latter conformation, C δ of I606 is only 2.3 Å away from C β of proline, producing a sterical clash and explaining the low efficiency of OphP towards substrates with a proline at the P1 site.

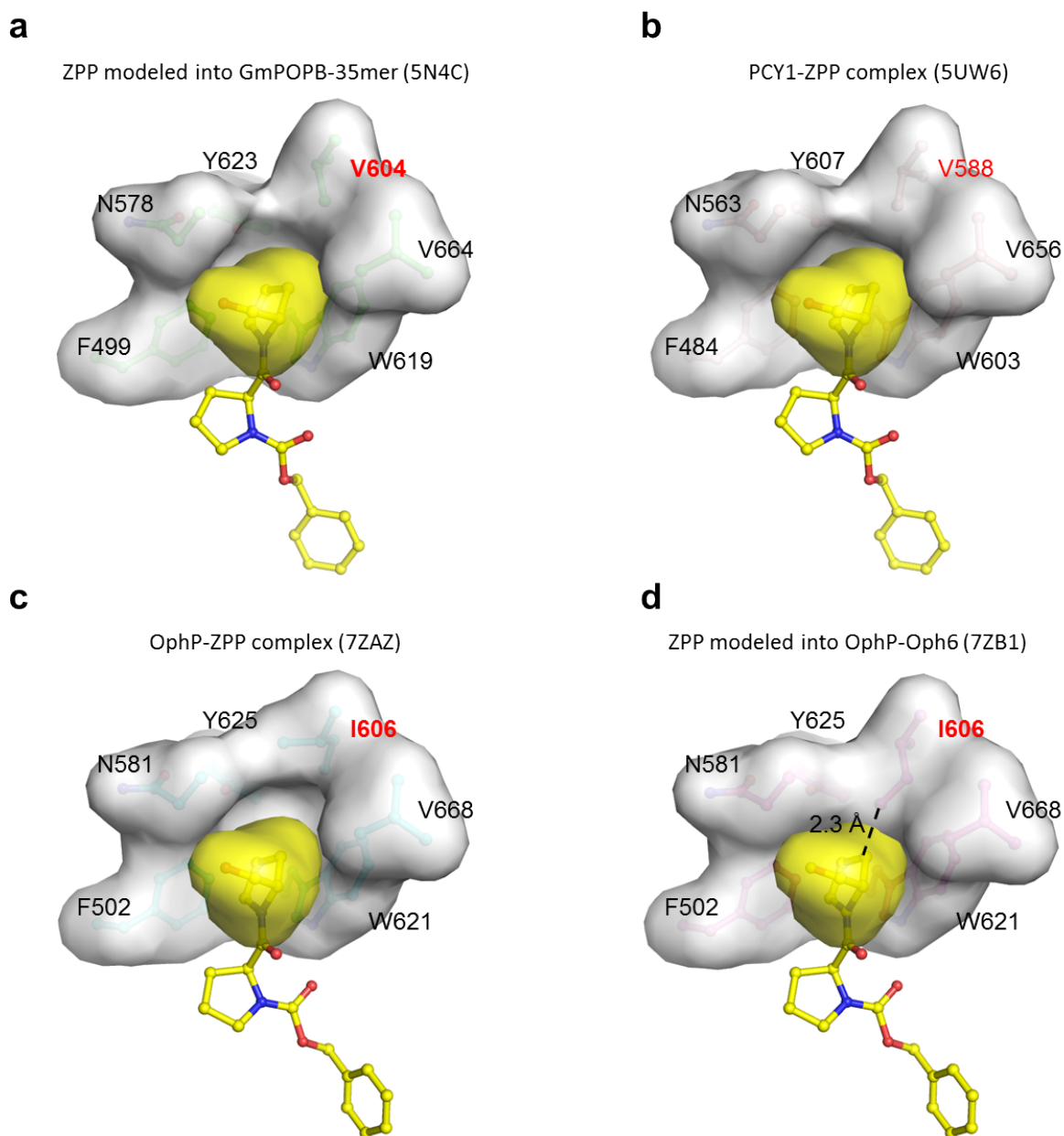


Figure S19. Crystal structures of OphP in complex with Oph-5. σ_A -weighted 2mFo-DFc map (contoured at 1) for Oph-5 (a) complexed with OphP S580A. Active site view of OphP: Oph-5 (b) in the complex structure showing the interactions. Side chains of the active site residues are shown in sticks with carbon green, nitrogen blue, oxygen red and the methyl groups orange. Broken lines show hydrogen bonds.

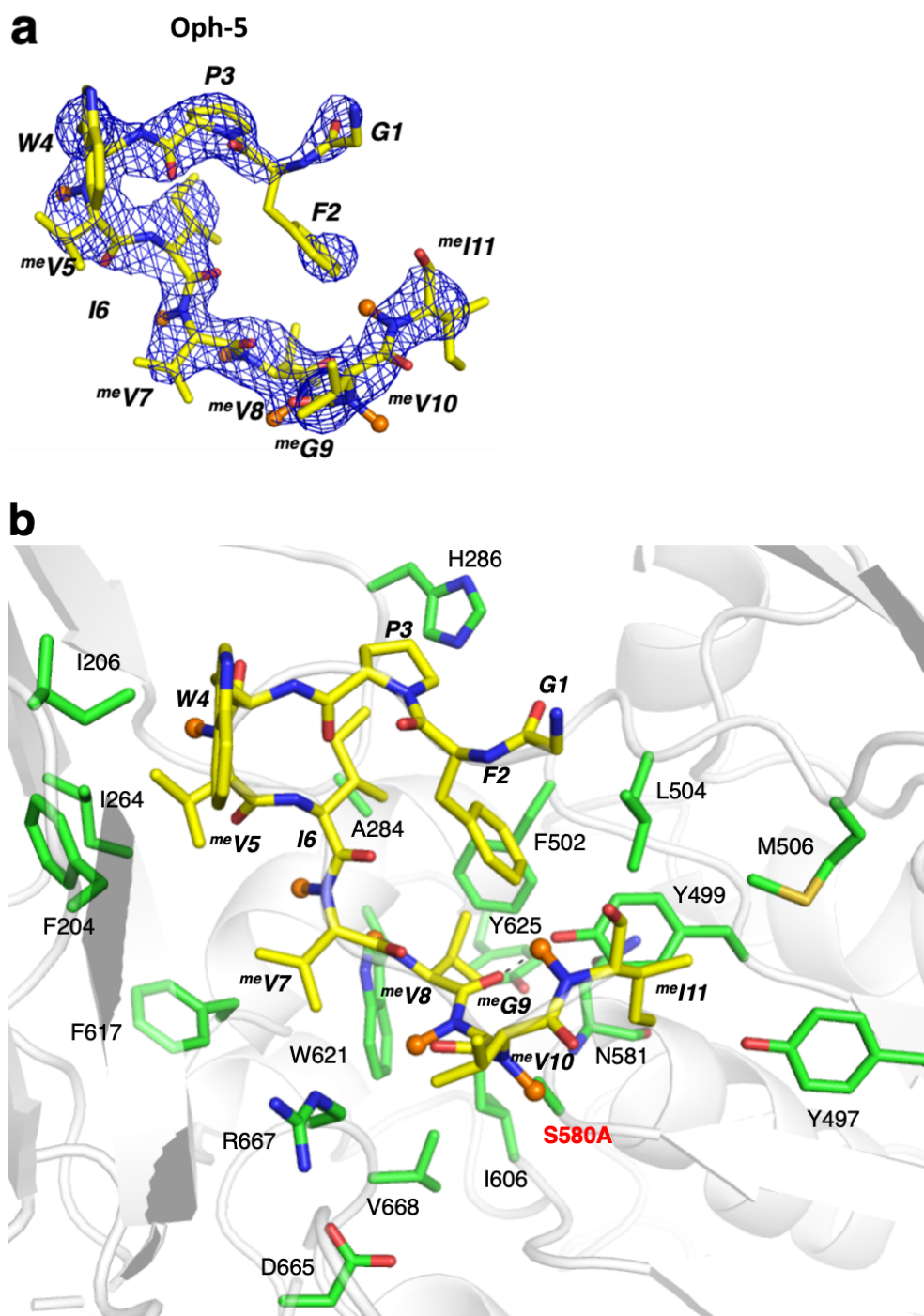


Figure S20. ITC experiments between OphP(S580A) and residues from the clasp domain (MPSSLLDAARESGEEASQNGFP), follower peptide (SVMSTE, and VIGSVMSTE), and Oph-5. Residues from the clasp domain (a) and follower peptides (b and c) showed no binding up to 2 mM in the presence of 50 μ M of OphP(S580A). Oph-5 binds to OphP(S580A) with a K_D of 1.5 μ M (d). The positive value of ΔH showed that the binding is endothermic suggesting the exclusion of water solvent during binding.

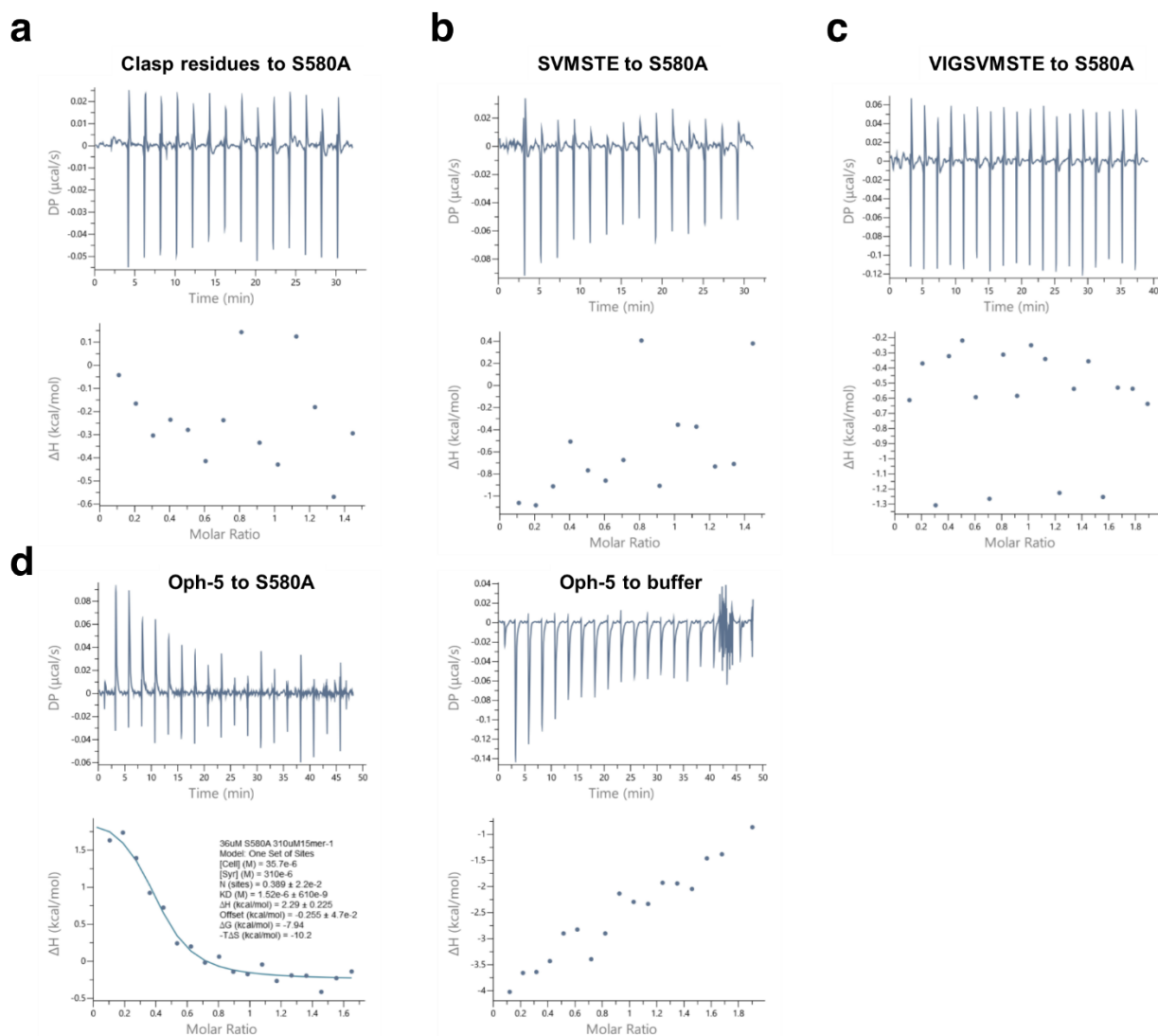
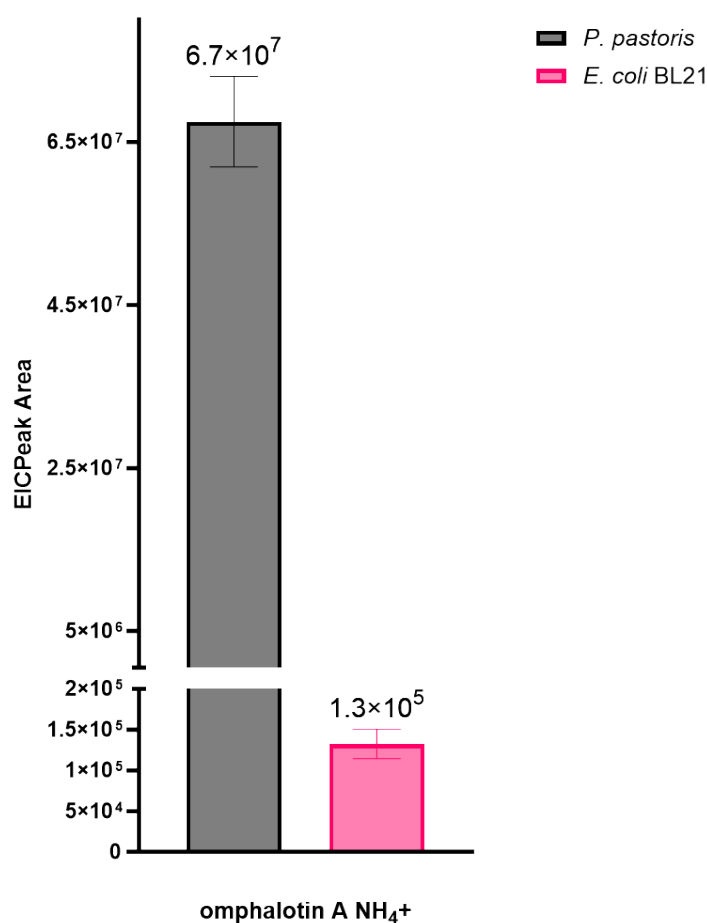


Figure S21. Production of omphalotin A in *P. pastoris* and *E. coli*. Production of omphalotin A in *P. pastoris* was performed as described previously^[2,4]. In *E. coli*, production of omphalotin A was attempted by co expression of *ophMA* and *ophP* under the control of a T7 promoter. *E. coli* was grown in TB medium until OD₆₀₀ 1.5 and expression was induced by addition of 0.2 mM IPTG. The induced cultures were incubated for five days at 16 °C. The bacterial cells were lysed using 0.1 mm glass beads in a FastPrep device and omphalotin A was extracted using a 1:1 mixture of ethyl acetate and n-hexane. The organic phase was evaporated, the pellets were redissolved in 100 µl of methanol and 10 µl of the solution was subjected to HPLC-MS/MS analysis. The graph shows the extracted ion chromatogram (EIC) peak area of omphalotin A extracted from *P. pastoris* and *E. coli* adjusted to culture volume.



References

- [1] C. M. Czekster, H. Ludewig, S. A. McMahon, J. H. Naismith, *Nat. Commun.* **2017**, *8*, 1045.
- [2] E. Matabaro, H. Song, C. Chepkirui, H. Kaspar, L. Witte, J. H. Naismith, M. F. Freeman, M. Künzler, *Methods Enzymol.* **2021**, *656*, 429–458.
- [3] H. Song, N. S. Van Der Velden, S. L. Shiran, P. Bleiziffer, C. Zach, R. Sieber, A. S. Imani, F. Krausbeck, M. Aebi, M. F. Freeman, M. Künzler, J. H. Naismith, *Sci. Adv.* **2018**, *4*, 2720.
- [4] E. Matabaro, H. Kaspar, P. Dahlin, D. L. V Bader, C. E. Murar, F. Staubli, C. M. Field, J. W. Bode, M. Künzler, *Sci. Rep.* **2021**, *11*, 3541.
- [5] H. Luo, S.-Y. Hong, R. M. Sgambelluri, E. Angelos, X. Li, J. D. Walton, *Chem. Biol.* **2014**, *21*, 1610–1617.